Sirtuin 1 inhibition delays cyst formation in autosomal-dominant polycystic kidney disease

Xia Zhou,[1,2] Lucy X. Fan,[1,2] William E. Sweeney Jr.,[3] John M. Denu,[4] Ellis D. Avner,[3] and Xiaogang Li[1,2,5]

[1]Department of Internal Medicine and [2]Kidney Institute, University of Kansas Medical Center, Kansas City, Kansas, USA. [3]Department of Pediatrics, Medical College of Wisconsin, Milwaukee, Wisconsin, USA. [4]Department of Biomolecular Chemistry, University of Wisconsin, Madison, Wisconsin, USA. [5]Department of Biochemistry and Molecular Biology, University of Kansas Medical Center, Kansas City, Kansas, USA.

Autosomal-dominant polycystic kidney disease (ADPKD) is caused by mutations in either *PKD1* or *PKD2* and is characterized by the development of multiple bilateral renal cysts that replace normal kidney tissue. Here, we used *Pkd1* mutant mouse models to demonstrate that the nicotinamide adenine dinucleotide–dependent (NAD-dependent) protein deacetylase sirtuin 1 (SIRT1) is involved in the pathophysiology of ADPKD. SIRT1 was upregulated through c-MYC in embryonic and postnatal *Pkd1*-mutant mouse renal epithelial cells and tissues and could be induced by TNF-α, which is present in cyst fluid during cyst development. Double conditional knockouts of *Pkd1* and *Sirt1* demonstrated delayed renal cyst formation in postnatal mouse kidneys compared with mice with single conditional knockout of *Pkd1*. Furthermore, treatment with a pan-sirtuin inhibitor (nicotinamide) or a SIRT1-specific inhibitor (EX-527) delayed cyst growth in *Pkd1* knockout mouse embryonic kidneys, *Pkd1* conditional knockout postnatal kidneys, and *Pkd1* hypomorphic kidneys. Increased SIRT1 expression in *Pkd1* mutant renal epithelial cells regulated cystic epithelial cell proliferation through deacetylation and phosphorylation of Rb and regulated cystic epithelial cell death through deacetylation of p53. This newly identified role of SIRT1 signaling in cystic renal epithelial cells provides the opportunity to develop unique therapeutic strategies for ADPKD.

Introduction

Autosomal-dominant polycystic kidney disease (ADPKD), one of the most common genetic disorders in humans, is caused by mutations in *PKD1* (accounting for 85%–95% of cases) and *PKD2* (accounting for most of the remainder), which encode polycystin-1 (PC1) and polycystin-2 (PC2), respectively (1). The hallmark of the disease is the development of multiple bilateral renal cysts that replace normal kidney tissue, resulting in end-stage renal failure in approximately 50% of individuals with ADPKD. Cyst formation is thought to start early in development and to continue throughout the entire life of the affected individual. The cell biology of cyst formation/expansion in ADPKD involves a combination of hyperproliferation, dedifferentiation, and fluid secretion. This cystic transformation occurs in all nephron segments (2, 3). The primary molecular genetic basis for cyst formation appears to be homozygous loss of function, with somatic second hits occurring in the setting of a single inherited inactivating mutation (4, 5). Recent evidence indicates that epigenetic alterations that result in dysregulated intracellular signaling pathways may also promote cyst formation in ADPKD animal models (6).

SIRT1 is the most extensively studied member of a mammalian family of at least 7 unique proteins, the sirtuins, which were originally identified in yeast as a major family of nicotinamide adenine dinucleotide–dependent (NAD-dependent) protein deacetylases important for extending life span in model organisms (7). New data have identified multiple roles for this protein family, which appears to target proteins involved in regulating metabolism and stress response, transcription factors and cofactors, histones and other chromatin proteins, and components of the DNA repair machinery (8). Although many of the exact mechanisms of sirtuins remain unknown, it is clear that they play an important role in diseases in which there is altered metabolism and stress responses, such as neurodegenerative diseases, cancer, cardiovascular disease, and inflammation (7). SIRT1 has been found to modify and silence the transcription by histone deacetylation, which includes deacetylating histones H1 at Lys-26, H3K9, and H4K16 necessary to form heterochromatin (9). SIRT1 also deacetylates nonhistone proteins, such as transcriptional factors that include Rb, E2F1, p53, NF-κB, FOXO1, FOXO3, c-MYC, β-catenin, and SMAD7, to potentially regulate cell proliferation and apoptosis (8, 10–12). SIRT1 appears to function by removing an acetyl group from acetylated lysine residues and thus generates lysine, 2′-O-acetyl-ADP-ribose (OAADPr), and nicotinamide (vitamin B3). By promoting a base-exchange reaction at the expense of deacetylation, nicotinamide serves as a noncompetitive inhibitor of SIRT1 (13, 14). Although SIRT1 has been reported to be involved in a variety of diseases, no previous studies have implicated SIRT1 and the sirtuin family in the pathophysiology of ADPKD. In this study, we examined the functional roles of SIRT1 and SIRT1-mediated protein deacetylation in the pathogenesis of ADPKD. Our findings provide a molecular basis for the potential use of nicotinamide to delay cyst formation in ADPKD patients.

Results

SIRT1 is upregulated in Pkd1 mutant renal epithelial cells and tissues. To initiate our studies on the functional role of SIRT1 in ADPKD, we examined mRNA and protein levels of SIRT1 in *Pkd1* mutant renal epithelial cells and kidneys. We found that mRNA and protein expression of SIRT1 was increased in *Pkd1*-null versus WT control mouse embryonic kidney (MEK) cells and in the postnatal

Authorship note: Xia Zhou and Lucy X. Fan contributed equally to this work.
Conflict of interest: The authors have declared that no conflict of interest exists.
Citation for this article: *J Clin Invest.* 2013;123(7):3084–3098. doi:10.1172/JCI64401.

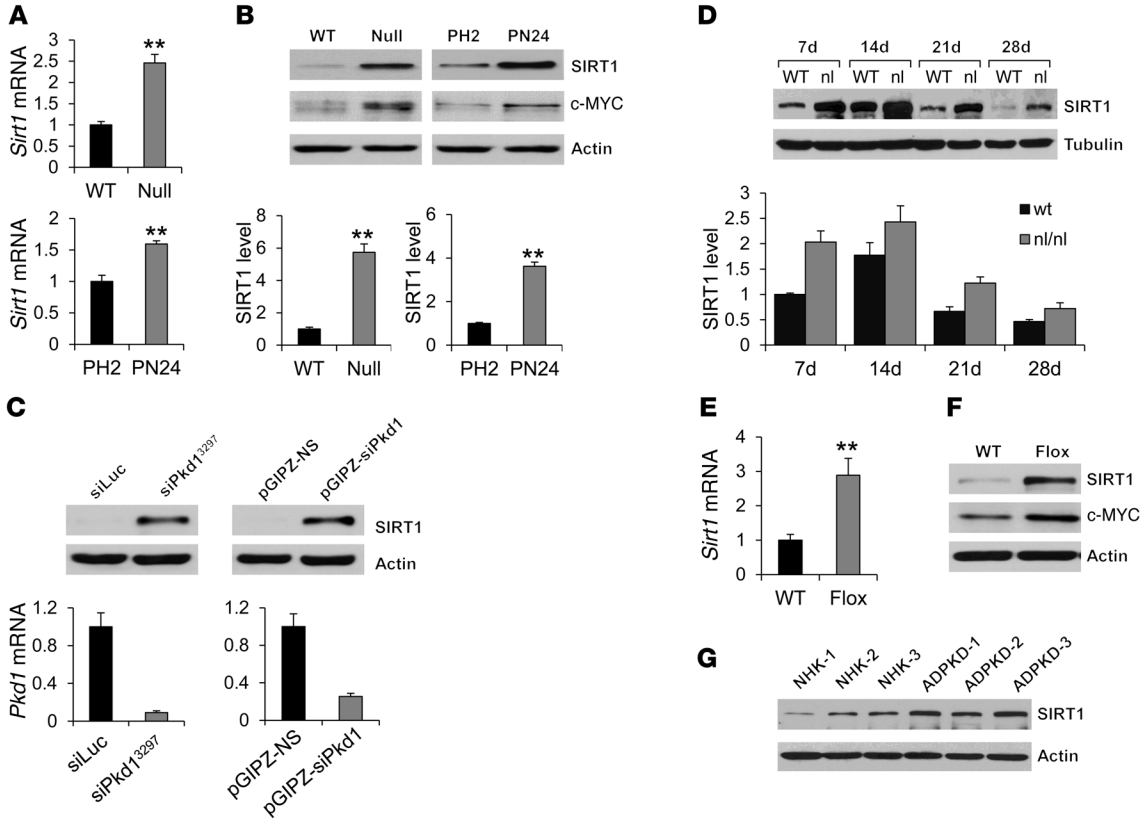

Figure 1

Pkd1-mutant renal epithelial cells and tissues demonstrated increased expression of SIRT1. (**A**) qRT-PCR analysis of relative *Sirt1* mRNA expression in WT MEK (WT), *Pkd1*-null MEK (Null), PH2, and PN24 cells. (**B**) Top: Western blot analysis of SIRT1 and c-MYC expression from whole cell lysates. Bottom: Relative SIRT1 expression, quantified from 3 independent immunoblots and standardized to actin. (**C**) Top: Western blot analysis of SIRT1 expression in mouse IMCD3 cells with *Pkd1* knockdown by 2 different lentivector-mediated *Pkd1* shRNAs, VIRHD/P/siPkd1^{3297} (siPKD1^{3297}) and pGIPZ-siPkd1, compared with that in the cells transduced with the respective control vectors, VIRHD/P/siLuc and pGIPZ-NS. Bottom: Relative *Pkd1* knockdown efficiency, evaluated by qRT-PCR, indicated that *Pkd1* expression was reduced by more than 90% and 70% in VIRHD/P/siPKD1^{3297}– and pGIPZ-siPkd1–transduced mouse IMCD3 cells, respectively, compared with that in control vector–transduced cells. (**D**) Top: Western blot analysis of SIRT1 expression in kidneys from WT and *Pkd1*$^{nl/nl}$ mice collected at P7, P14, P21, and P28. Bottom: Relative SIRT1 expression in the kidneys, standardized to tubulin. (**E** and **F**) qRT-PCR analysis of *Sirt1* mRNA expression (**E**) and Western blot analysis of SIRT1 and c-MYC expression (**F**) in P7 kidneys from *Pkd1*$^{+/+}$*:Ksp-Cre* (WT) and *Pkd1*$^{flox/flox}$*:Ksp-Cre* (Flox) neonates. (**G**) Western blot analysis of SIRT1 expression in primary human ADPKD and NHK cells. $^{**}P < 0.01$.

Pkd1-null cell line PN24 compared with the postnatal *Pkd1*-heterozygous cell line PH2 (Figure 1, A and B). Knockdown of *Pkd1* with 2 different lentivirus-mediated shRNAs in mouse inner medullary collecting duct (IMCD3) cells also resulted in upregulation of SIRT1 relative to appropriate controls (Figure 1C). SIRT1 expression was also increased in kidneys from well-characterized hypomorphic homozygous *Pkd1*$^{nl/nl}$ mice (15) compared with that in age-matched WT kidneys at P7, P14, P21, and P28 (Figure 1D). In addition, mRNA and protein expression of SIRT1 increased in P7 kidneys of *Pkd1*$^{flox/flox}$*:Ksp-Cre* mice, as analyzed by quantitative RT-PCR (qRT-PCR), Western blot, and immunohistochemistry (Figure 1, E and F, and Supplemental Figure 1A; supplemental material available online with this article; doi:10.1172/JCI64401DS1). Furthermore, SIRT1 expression was upregulated in primary human ADPKD cells and ADPKD kidneys compared with primary normal human kidney (NHK) cells and normal kidneys, respectively (Figure 1G and Supplemental Figure 1B). These results suggest that the increased expression of SIRT1 in renal epithelial cells is caused by loss or mutation of *Pkd1*.

PC1 affects SIRT1 expression in renal epithelial cells through c-MYC. It has been reported that in ADPKD, renal c-MYC expression is elevated up to 15-fold (16). c-MYC has been shown to regulate SIRT1 expression in human cancer (HeLa) cells (17). Thus, c-MYC may regulate SIRT1 expression in renal epithelial cells. In support of this notion, we found that (a) c-MYC expression was increased in *Pkd1*-null MEK cells, PN24 cells, and kidney tissues from *Pkd1*$^{flox/flox}$*:Ksp-Cre* mice (Figure 1, B and F); (b) overexpression of c-MYC increased mRNA and protein levels of SIRT1 in WT MEK cells and PH2 cells (Figure 2, A and B); (c) knockdown of c-MYC with siRNA decreased mRNA and protein levels of SIRT1 in *Pkd1*-null MEK cells and PN24 cells (Figure 2, C and D); and (d) c-MYC bound to 2 potential c-MYC–binding sites (E-boxes E1 and E2; ref. 18) of the SIRT1 promoter, as determined by ChIP assay with anti–c-MYC antibody (Figure 2E). These results suggested that loss of PC1 mechanistically altered SIRT1 expression in renal epithelial cells through c-MYC.

SIRT1 expression can be further induced by TNF-α in Pkd1 mutant renal epithelial cells. TNF-α, which is detected in cyst fluid and promotes cyst formation (19), has been found to induce SIRT1 expres-

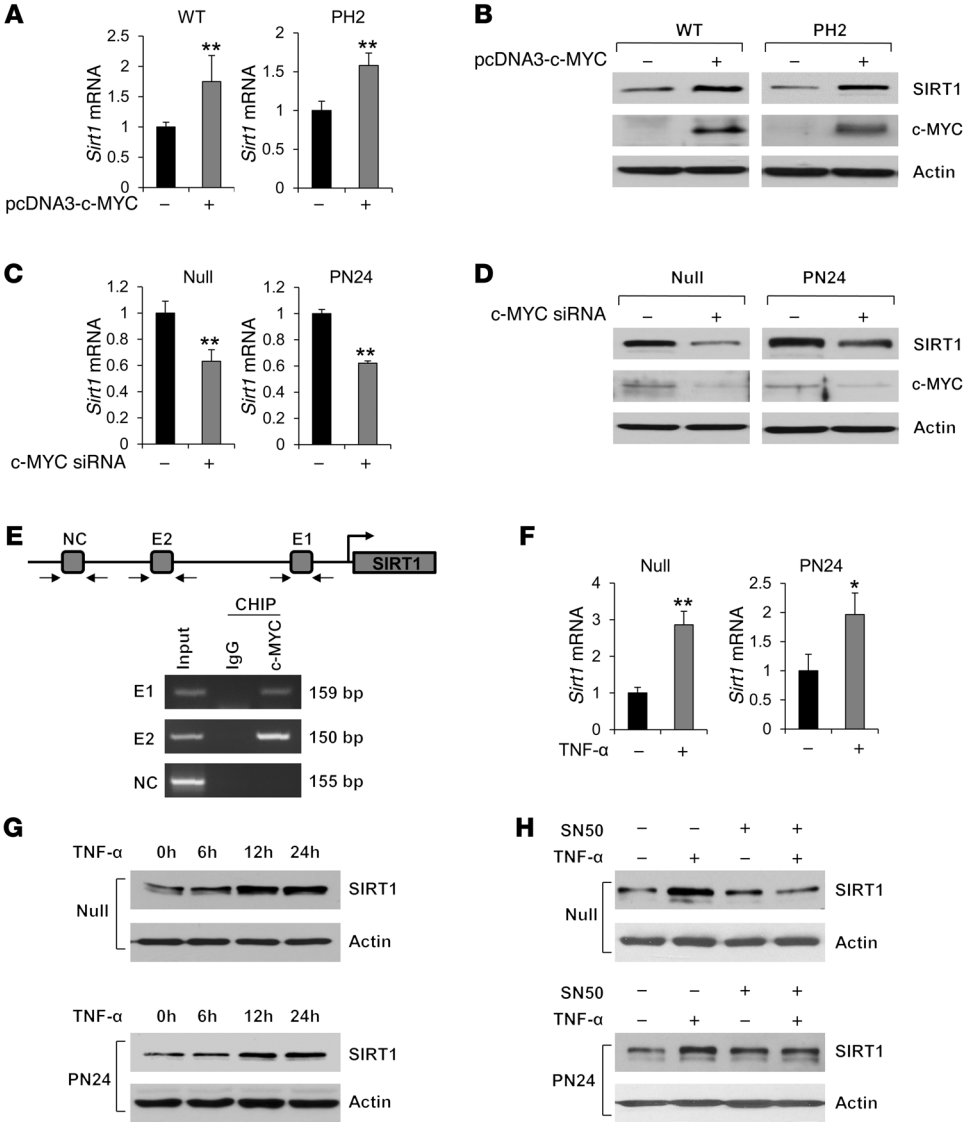

Figure 2
SIRT1 expression is regulated by c-MYC and is induced by TNF-α. (**A** and **B**) Overexpression of c-MYC increased levels of (**A**) *Sirt1* mRNA, as analyzed by qRT-PCR, and (**B**) SIRT1 protein, as analyzed by Western blot, in WT MEK cells and PH2 cells transfected with pcDNA3-c-MYC for 48 hours. (**C** and **D**) Knockdown of c-MYC with siRNA decreased the levels of (**C**) *Sirt1* mRNA, as analyzed by qRT-PCR, and (**D**) SIRT1 protein, as analyzed by Western blot, in *Pkd1*-null MEK cells and PN24 cells transfected with c-MYC siRNA for 48 hours. (**E**) c-MYC bound to the promoter of SIRT1. CHIP assay was performed with anti–c-MYC antibody or normal rabbit IgG in *Pkd1*-null MEK cells. The precipitated chromatin DNA was analyzed by PCR with primers that amplified from –1,009 to –850 bp (E1) or from –2,535 to –2,385 bp (E2). The PCR amplification for distant regions (–3,178 to –3,023 bp) was used as a negative control (NC). (**F** and **G**) TNF-α (100 ng/ml) induced (**F**) *Sirt1* mRNA, as detected by qRT-PCR, and (**G**) SIRT1 protein, as detected by Western blot, in *Pkd1*-null MEK cells and PN24 cells. (**H**) Western blot analysis of SIRT1 expression in *Pkd1*-null MEK cells and PN24 cells treated with TNF-α (100 ng/ml) and/or SN50 (50 μg/ml). $^{*}P < 0.05$; $^{**}P < 0.01$.

sion in vascular smooth muscle cells through the NF-κB p65/RelA subunit (20). We found that TNF-α induced mRNA and protein expression of SIRT1 in *Pkd1*-null MEK cells and PN24 cells (Figure 2, F and G). TNF-α also slightly induced SIRT1 expression in WT MEK cells, but had no effect in PH2 or mouse IMCD3 cells (Supplemental Figure 2). However, the NF-κB inhibitor SN50 efficiently blocked TNF-α–induced SIRT1 upregulation in *Pkd1*-null MEK cells and PN24 cells (Figure 2H), which suggests that TNF-α induces SIRT1 expression by activating the NF-κB pathway. Although it is unclear whether the cyst fluid TNF-α is initially secreted by immune cells or by cyst lining epithelial cells, these results suggest that the presence of TNF-α in cyst fluid during cyst development may serve as a secondary stimulus to further increase expression of SIRT1 in cyst lining epithelial cells in vivo.

Sirt1 and Pkd1 double conditional knockout delayed renal cyst formation. In order to explore the in vivo function of SIRT1 in a *Pkd1*-knockout mouse model, we crossed *Pkd1*$^{flox/+}$*:Sirt1*$^{flox/+}$*:Ksp-Cre* female mice with *Pkd1*$^{flox/+}$*:Sirt1*$^{flox/+}$*:Ksp-Cre* male mice, which have a kidney-specific Ksp-cadherin driving Cre expression. Cyst formation was significantly delayed in the absence of SIRT1 in *Pkd1*$^{flox/flox}$*:Sirt1*$^{flox/flox}$*:Ksp-Cre* mice at P7 compared with that in age-matched *Pkd1*$^{flox/flox}$*:Sirt1*$^{+/+}$*:Ksp-Cre* and *Pkd1*$^{flox/flox}$*:Sirt1*$^{flox/+}$*:Ksp-Cre* mice (n = 10 per group; Figure 3, A–E). Kidney weight/body weight (KW/BW) ratios from *Pkd1*$^{flox/flox}$*:Sirt1*$^{flox/flox}$*:Ksp-Cre* mice were dramatically reduced compared with *Pkd1*$^{flox/flox}$*:Sirt1*$^{+/+}$*:Ksp-Cre* mice (Figure 3F). In addition, blood urea nitrogen (BUN) levels were also significantly reduced in *Pkd1*$^{flox/flox}$*:Sirt1*$^{flox/flox}$*:Ksp-Cre* mice compared with *Pkd1*$^{flox/flox}$*:Sirt1*$^{+/+}$*:Ksp-Cre* mice (Figure 3G), which indicates that renal function was normalized in *Pkd1*$^{flox/flox}$*:Sirt1*$^{flox/flox}$*:Ksp-Cre* mice. At the same time, SIRT1 expression was not detected in cyst lining epithelial cells in kidneys from *Pkd1* and *Sirt1* double–conditional knockout mice, as analyzed by immunohistochemistry (Supplemental Figure 3). Proliferating cell nuclear antigen (PCNA) staining was used to determine the proliferation of cyst lining epithelial cells, which was significantly decreased in *Pkd1* and *Sirt1* double–conditional knockout versus *Pkd1* single–conditional knockout (i.e., *Sirt1*$^{+/+}$) renal epithelia (Figure 3H). Furthermore, we found that *Pkd1* and *Sirt1* double–

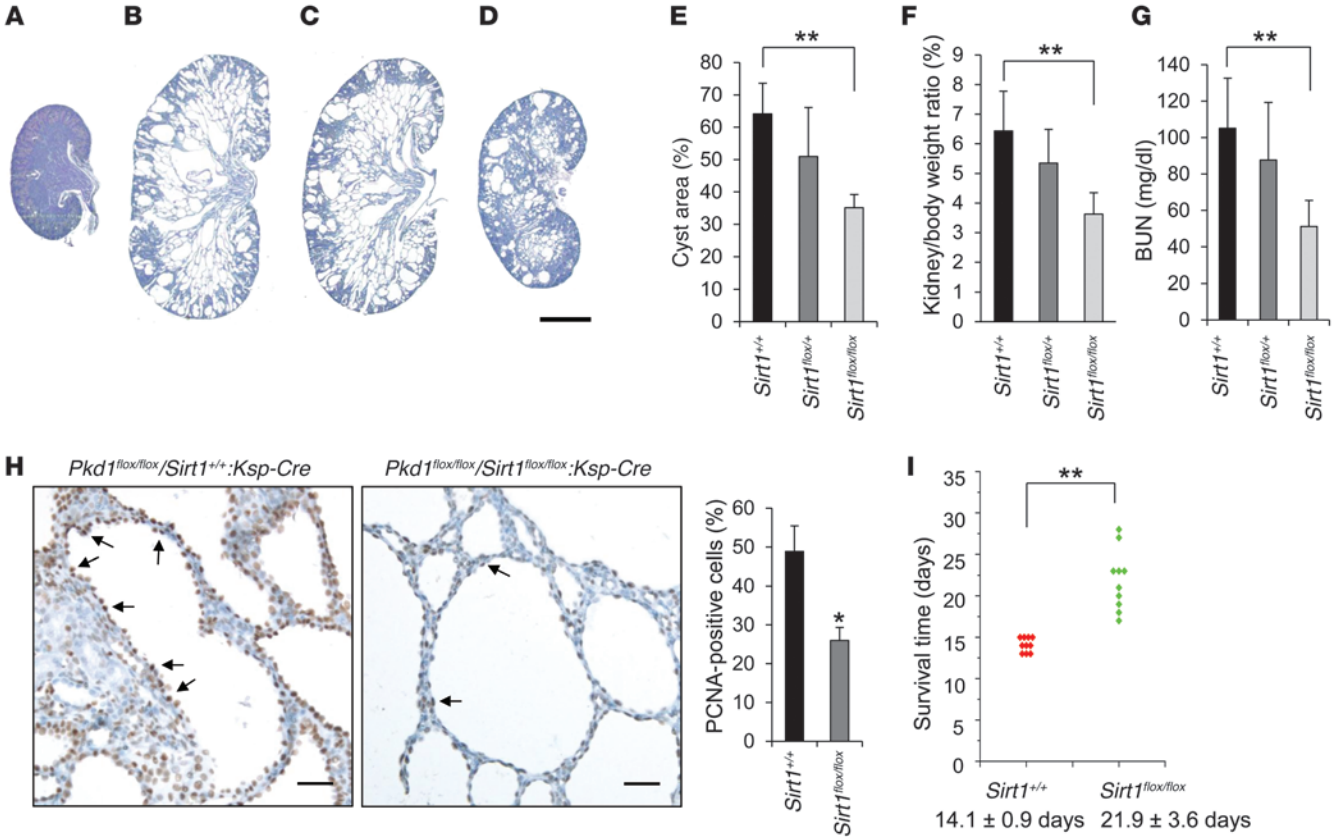

Figure 3

Double conditional knockout of *Sirt1* and *Pkd1* delayed renal cyst formation. (**A**–**D**) Histologic examination of P7 kidneys from (**A**) *Pkd1*$^{+/+}$*:Sirt1*$^{flox/flox}$*:Ksp-Cre*, (**B**) *Pkd1*$^{flox/flox}$*:Sirt1*$^{+/+}$*:Ksp-Cre*, (**C**) *Pkd1*$^{flox/flox}$*:Sirt1*$^{flox/+}$*:Ksp-Cre*, and (**D**) *Pkd1*$^{flox/flox}$*:Sirt1*$^{flox/flox}$*:Ksp-Cre* neonates. (**E**) Percent cystic area relative to total kidney section area was significantly decreased in P7 kidneys from *Pkd1*$^{flox/flox}$*:Sirt1*$^{flox/flox}$*:Ksp-Cre* (*Sirt1*$^{flox/flox}$) versus *Pkd1*$^{flox/flox}$*:Sirt1*$^{+/+}$*:Ksp-Cre* (*Sirt1*$^{+/+}$) neonates. Data reflect all sections quantified for each condition (n = 10 per group). (**F**) KW/BW ratios were dramatically reduced in P7 *Pkd1*$^{flox/flox}$*:Sirt1*$^{flox/flox}$*:Ksp-Cre* versus *Pkd1*$^{flox/flox}$*:Sirt1*$^{+/+}$*:Ksp-Cre* neonates. (**G**) BUN levels of P7 *Pkd1*$^{flox/flox}$*:Sirt1*$^{+/+}$*:Ksp-Cre*, *Pkd1*$^{flox/flox}$*:Sirt1*$^{flox/+}$*:Ksp-Cre*, and *Pkd1*$^{flox/flox}$*:Sirt1*$^{flox/flox}$*:Ksp-Cre* neonates. (**H**) Cell proliferation (arrows) was decreased in P7 *Pkd1*$^{flox/flox}$*:Sirt1*$^{flox/flox}$*:Ksp-Cre* versus *Pkd1*$^{flox/flox}$*:Sirt1*$^{+/+}$*:Ksp-Cre* neonate kidneys, as detected with PCNA staining. The percentage of PCNA-positive nuclei in cystic lining epithelial cells was calculated from an average of 1,000 nuclei per mouse kidney section; only strongly stained nuclei were considered PCNA-positive. (**I**) *Pkd1*$^{flox/flox}$*:Sirt1*$^{flox/flox}$*:Ksp-Cre* mice lived to 21.9 ± 3.6 days, whereas *Pkd1*$^{flox/flox}$*:Sirt1*$^{+/+}$*:Ksp-Cre* mice died of polycystic kidney disease at 14.1 ± 0.9 days. Scale bars: 2 mm (**A**–**D**); 30 μm (**H**). *P < 0.05; **P < 0.01.

conditional knockout mice lived to a mean age of 21.9 ± 3.6 days, while *Pkd1*$^{flox/flox}$*:Sirt1*$^{+/+}$*:Ksp-cre* mice died of polycystic kidney disease at 14.1 ± 0.9 days (P < 0.01; Figure 3I). Our in vivo data suggested that SIRT1 is involved in regulating renal cyst formation in *Pkd1*-knockout mice.

A pan-sirtuin inhibitor or a specific SIRT1 inhibitor delays cyst growth in Pkd1-mutant kidneys. To test whether inhibiting the activity of SIRT1 would suppress cyst formation in *Pkd1*$^{-/-}$ embryos, we injected nicotinamide into pregnant *Pkd1*$^{+/-}$ female mice from 7.5 dpc after mating with *Pkd1*$^{+/-}$ males, and analyzed MEKs at 15.5 dpc. We found that in all E15.5 *Pkd1*$^{-/-}$ embryos from nicotinamide-injected mothers, renal cyst formation was drastically reduced compared with kidneys of *Pkd1*$^{-/-}$ embryos from control DMSO-injected mothers (n = 10 per treatment group; P < 0.01; Figure 4, A–E). Furthermore, nicotinamide induced tubular epithelial cell apoptosis in kidneys from *Pkd1*$^{-/-}$ E15.5 embryos, while apoptosis was rare and negligible in kidneys from DMSO-treated *Pkd1*$^{-/-}$ E15.5 embryos (Figure 4F). We also evaluated the effect of nicotinamide on renal cyst formation at 18.5 dpc; indeed, renal cyst growth was dramatically reduced in kidneys of E18.5 *Pkd1*$^{-/-}$ embryos from nicotinamide- versus DMSO-injected pregnant females (n = 10 per treatment group; Figure 4, G and H). Kidney weight was also significantly decreased in *Pkd1*$^{-/-}$ embryos from nicotinamide-injected pregnant females (Figure 4I). Again, tubular epithelial cell apoptosis was induced by nicotinamide in E18.5 kidneys from *Pkd1*$^{-/-}$ embryos, but was rare in E18.5 kidneys from DMSO-treated *Pkd1*$^{-/-}$ embryos (Figure 4J). Furthermore, we found that treatment with nicotinamide increased the survival of *Pkd1*$^{-/-}$ E18.5 embryos compared with those treated with DMSO (P < 0.01; Supplemental Table 1).

Next, we tested whether nicotinamide or EX-527, a specific SIRT1 inhibitor (21), could reduce cyst initiation or growth in *Pkd1*$^{flox/flox}$*:Ksp-Cre* mice. Cyst progression is aggressive in the kidneys of *Pkd1*$^{flox/flox}$*:Ksp-Cre* mice (22), which allowed us to examine the effect of nicotinamide on initiation and progressive enlargement of cyst formation. *Pkd1*$^{flox/flox}$*:Ksp-Cre* pups were injected i.p. with

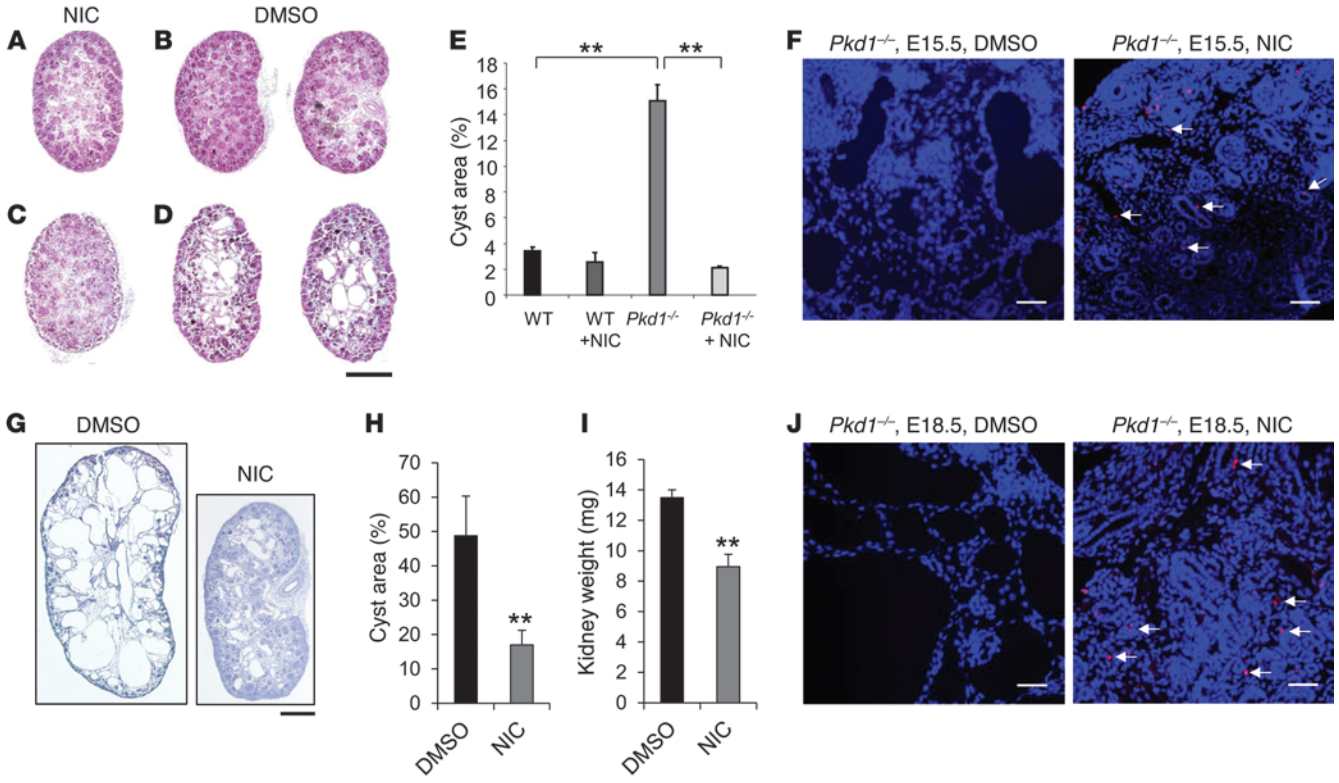

Figure 4
Nicotinamide treatment delayed cyst formation in *Pkd1*$^{-/-}$ MEKs. (**A**–**D**) Histological examination of E15.5 WT and *Pkd1*$^{-/-}$ MEKs from pregnant females injected daily with nicotinamide (NIC) or DMSO vehicle control from 7.5 to 14.5 dpc. (**A**) Nicotinamide-treated WT. (**B**) DMSO-treated WT. (**C**) Nicotinamide-treated *Pkd1*$^{-/-}$. (**D**) DMSO-treated *Pkd1*$^{-/-}$. (**E**) Percent cystic area relative to total kidney section area of E15.5 kidneys from WT and *Pkd1*$^{-/-}$ embryos treated with nicotinamide or DMSO (n = 10 per treatment group). For all mice, the middle section of each kidney was quantified. (**F**) Nicotinamide induced cyst lining epithelial cell death (arrows) in *Pkd1*$^{-/-}$ E15.5 MEKs, while apoptosis was rare in DMSO-treated *Pkd1*$^{-/-}$ E15.5 MEKs, as detected by TUNEL assay. (**G**) Histological examination of E18.5 *Pkd1*$^{-/-}$ MEKs from pregnant females injected daily with DMSO or nicotinamide from 7.5 to 17.5 dpc. (**H**) Percent cystic area relative to total kidney section area of E18.5 kidneys from *Pkd1*$^{-/-}$ embryos treated with DMSO or nicotinamide (n = 10 per treatment group). (**I**) Kidney weight of *Pkd1*$^{-/-}$ E18.5 kidneys from pregnant females treated with DMSO or nicotinamide (n = 10 per treatment group). (**J**) Nicotinamide induced cyst lining epithelial cell death (arrows) in *Pkd1*$^{-/-}$ E18.5 kidneys, while apoptosis was rare in DMSO-treated *Pkd1*$^{-/-}$ E18.5 kidneys, as detected by TUNEL assay. Scale bars: 500 μm (**A**–**D** and **G**); 20 μm (**F** and **J**). $^{**}P < 0.01$.

nicotinamide (0.25 mg/g), EX-527 (2 mg/kg) or DMSO daily from P3 to P6, and kidneys were harvested and analyzed at P7. Administration of nicotinamide or EX-527 during this early phase delayed renal cyst growth ($P < 0.01$; Figure 5, A and B), inhibited cystic epithelial cell proliferation (PCNA staining; Figure 5E), and induced cystic epithelial cell apoptosis (TUNEL assay; Supplemental Figure 4A) in P7 kidneys from *Pkd1*$^{flox/flox}$:*Ksp-Cre* mice compared with DMSO injection (n = 10 per treatment group). KW/BW ratios and BUN levels in *Pkd1*$^{flox/flox}$:*Ksp-Cre* mice were dramatically reduced by nicotinamide or EX-527 treatment compared with DMSO treatment (Figure 5, C and D). Additionally, gender did not influence cyst formation and progression, as determined by comparing 5 male mice and 5 female *Pkd1*$^{flox/flox}$:*Ksp-Cre* mice per treatment group with respect to cystic index and KW/BW ratios. To further confirm that nicotinamide delayed cyst formation by specifically targeting SIRT1, we treated *Pkd1*$^{flox/flox}$:*Sirt1*$^{flox/flox}$:*Ksp-Cre* mice with nicotinamide daily from P3 to P6 and collected the kidneys at P7. The rationale for this experiment was that if nicotinamide delays cyst growth in *Pkd1* mutant mice by targeting SIRT1, then it will not affect cyst growth in *Pkd1*$^{flox/flox}$:*Sirt1*$^{flox/flox}$:*Ksp-Cre* mice, which lack SIRT1. We found that nicotinamide treatment did not further delay cyst growth in P7 kidneys of *Pkd1*$^{flox/flox}$:*Sirt1*$^{flox/flox}$:*Ksp-Cre* mice (n = 10 per treatment group; Supplemental Figure 4, B–D). These results demonstrated that nicotinamide delayed cyst growth by specifically inhibiting SIRT1 in the *Pkd1*$^{flox/flox}$:*Ksp-Cre* mice.

Finally, we examined whether nicotinamide or EX-527 could delay cyst growth in the progressive hypomorphic *Pkd1*$^{nl/nl}$ mouse model (15). *Pkd1*$^{nl/nl}$ pups were injected i.p. with nicotinamide (0.25 mg/g), EX-527 (2 mg/kg), or DMSO daily from P5 to P27, and kidneys were harvested and analyzed at P28. Administration of nicotinamide or EX-527 delayed cyst progression (Figure 6, A and B), inhibited cystic epithelial cell proliferation (Figure 6E), and induced cystic epithelial cell apoptosis (Supplemental Figure 5) in P28 *Pkd1*$^{nl/nl}$ kidneys compared with kidneys of age-matched DMSO-injected *Pkd1*$^{nl/nl}$ mice (n = 10 per treatment group). Nicotinamide or EX-527 treatment also significantly decreased KW/BW ratios and BUN levels in *Pkd1*$^{nl/nl}$ mice compared with DMSO injection (Figure 6, C and D). We also found that gender did not affect cyst formation and progression in *Pkd1*$^{nl/nl}$ mice by compar-

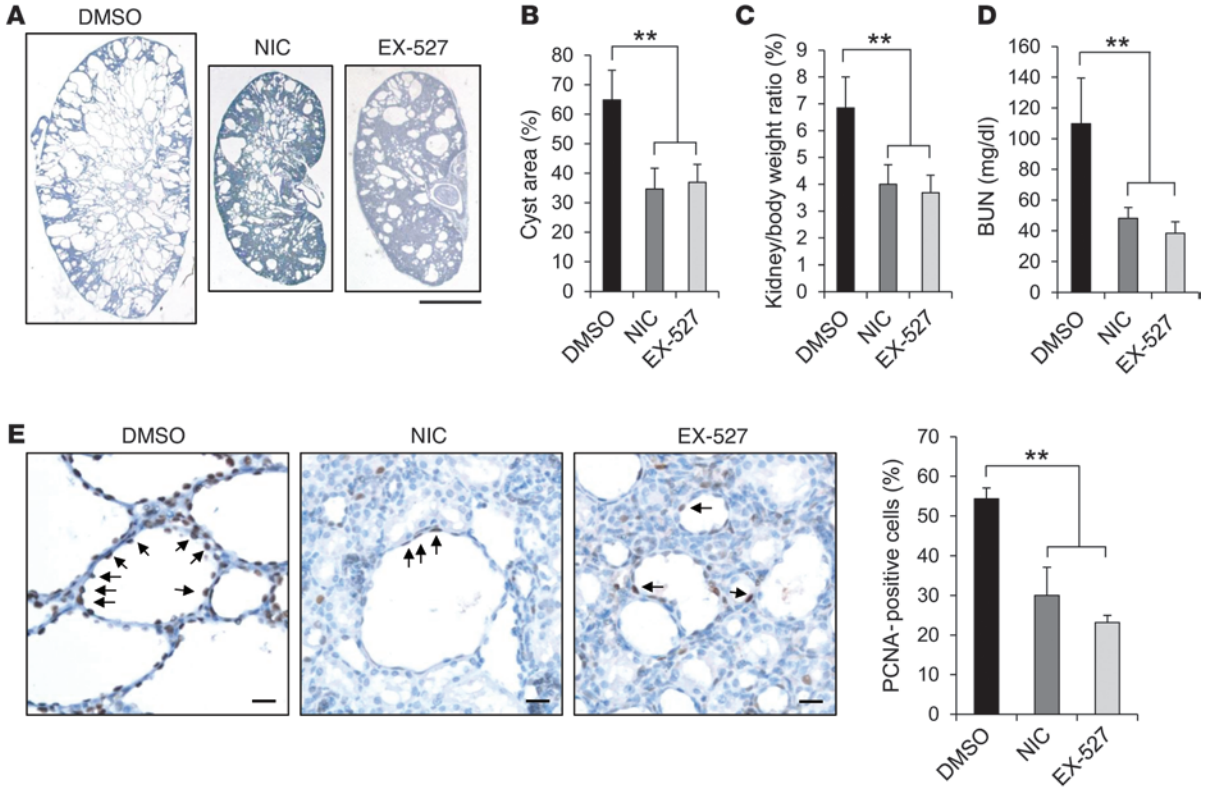

Figure 5

Treatment with nicotinamide or EX-527 delayed cyst growth in *Pkd1*$^{flox/flox}$*:Ksp-Cre* neonates. (**A**) Histologic examination of P7 kidneys from *Pkd1*$^{flox/flox}$*:Ksp-Cre* neonates treated with DMSO, nicotinamide, or EX-527 (n = 10 per treatment group). (**B**) Percent cystic area relative to total kidney section area of P7 kidneys from *Pkd1*$^{flox/flox}$*:Ksp-Cre* neonates treated as in **A**. Data reflect all sections quantified for each condition. (**C** and **D**) KW/BW ratios (**C**) and BUN levels (**D**) were decreased in *Pkd1*$^{flox/flox}$*:Ksp-Cre* P7 neonates treated with nicotinamide or EX-527 compared with DMSO treatment. (**E**) Nicotinamide and EX-527 treatment reduced cyst lining epithelial cell proliferation (arrows) in *Pkd1*$^{flox/flox}$*:Ksp-Cre* P7 kidneys, as detected by PCNA staining. Scale bars: 2 mm (**A**); 20 μm (**E**). $^{**}P < 0.01$.

ing 5 male mice and 5 female mice per group. These results further supported the notion that targeting SIRT1 with pharmacological inhibitors may delay cyst growth in ADPKD patients.

Silence or inhibition of SIRT1 decreases renal epithelial cell growth, but increases apoptosis. Our findings that genetic deletion of *Sirt1* or inhibition of SIRT1 with nicotinamide or EX-527 in *Pkd1*-mutant background mice not only delayed cyst formation, but also decreased cystic epithelial cell proliferation and increased cystic epithelial cell apoptosis, suggested that SIRT1-mediated downstream pathways are involved in this process. To support this notion, we examined the effect of SIRT1 overexpression and SIRT1 depletion or inhibition on cell proliferation with a BrdU proliferation assay in mouse IMCD3 cells and *Pkd1*-null renal epithelial cells, respectively. We found that overexpressing HA-tagged WT SIRT1, but not the deacetylase catalytically inactive mutant SIRT1-H355A (23), increased BrdU incorporation in mouse IMCD3 cells (Figure 7A). In contrast, knockdown of SIRT1 with siRNA decreased BrdU incorporation in *Pkd1*-null MEK cells and PN24 cells (Figure 7, B and C). In addition, treatment with different concentrations of nicotinamide resulted in a dose-dependent decrease in BrdU incorporation in *Pkd1*-null MEK cells and PN24 cells (Figure 7, D and E). These results suggest that upregulation of SIRT1 increases S-phase entry in *Pkd1*-mutant renal epithelial cells.

Next, we examined whether nicotinamide had a proapoptotic effect on WT MEK, *Pkd1*-null MEK, PH2, and PN24 cells by TUNEL assay. Nicotinamide induced apoptosis in *Pkd1*-null MEK cells and PN24 cells, but not in WT MEK cells or PH2 cells (Supplemental Figure 6, A and B). Flow cytometry analysis demonstrated that apoptosis was significantly increased in *Pkd1*-null MEK cells and PN24 cells treated with nicotinamide compared with vehicle (Figure 7, F and G). We further found that treatment with nicotinamide markedly increased the level of active caspase-3 in *Pkd1*-null MEK cells and PN24 cells, but not that in WT MEK cells or PH2 cells (Figure 7H). Caspase-3 activation was confirmed by the appearance of cleaved poly(ADP-ribose) polymerase (PARP), a substrate of caspase-3 (Figure 7H), which suggests that caspase-3 is the downstream executioner of nicotinamide-induced apoptosis in *Pkd1*-mutant renal epithelial cells.

SIRT1 regulates cystic epithelial cell proliferation by altering Rb acetylation and phosphorylation. Previous studies demonstrated that acetylation of Rb inhibits its phosphorylation by cyclin-dependent kinases and that SIRT1-mediated deacetylation of Rb increases its phosphorylation in vitro (12, 24). However, whether endogenous SIRT1 regulates Rb activity through this process is unknown. We demonstrated that knockdown of *Pkd1* in mouse IMCD3 cells with 2 different lentiviruses expressing shRNAs increased not only SIRT1 expression (Figure 1C), but also Rb phosphorylation (Figure 8A), compared with

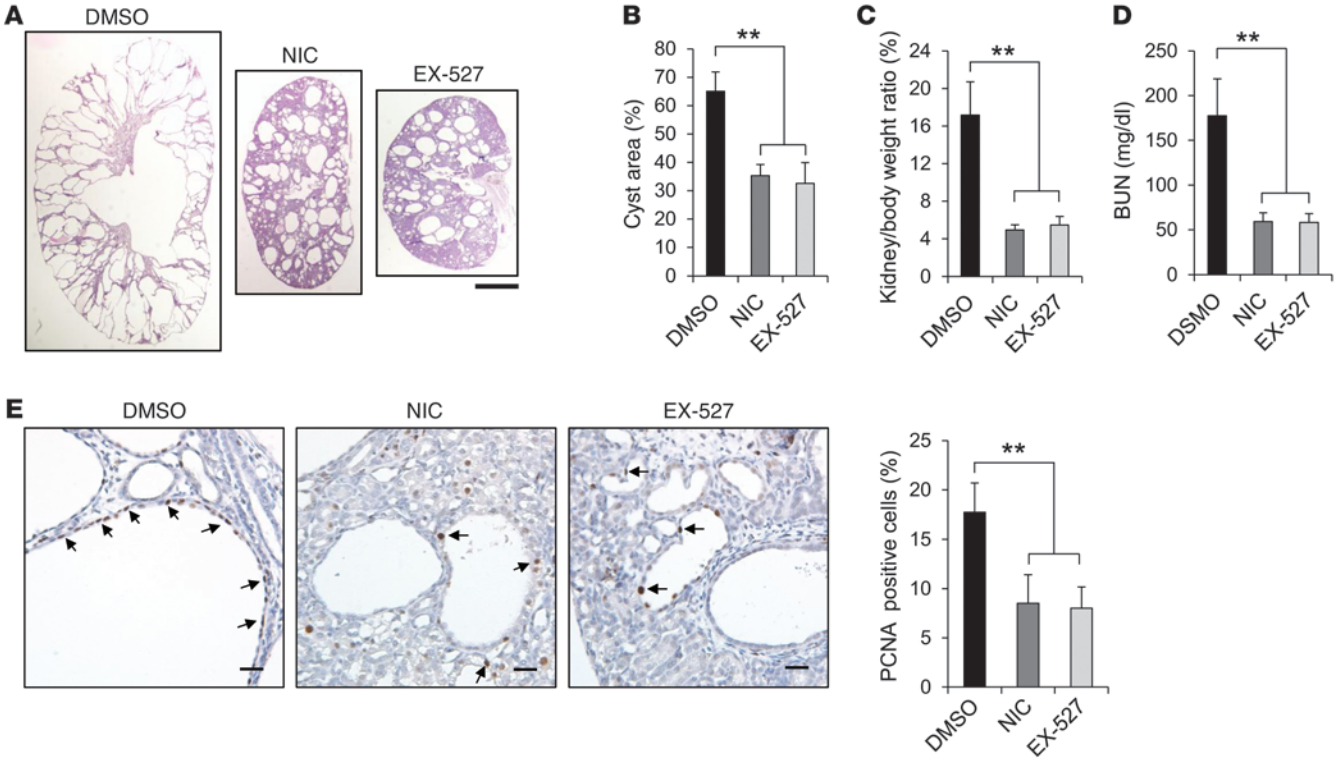

Figure 6
Treatment with nicotinamide or EX-527 delayed cyst growth in *Pkd1*$^{nl/nl}$ mice. (**A**) Histologic examination of P28 kidneys from *Pkd1*$^{nl/nl}$ mice treated with DMSO, nicotinamide, or EX-527 (n = 10 per treatment group). (**B**) Percent cystic area relative to total kidney section area of P28 kidney sections from *Pkd1*$^{nl/nl}$ mice treated as in **A**. Data reflect all sections quantified for each condition. (**C** and **D**) KW/BW ratios (**C**) and BUN levels (**D**) were decreased in P28 *Pkd1*$^{nl/nl}$ mice treated with nicotinamide or EX-527 compared with DMSO treatment. (**E**) Nicotinamide and EX-527 treatment reduced cyst lining epithelial cell proliferation (arrows) in P28 kidneys from *Pkd1*$^{nl/nl}$ mice, as detected by PCNA staining. Scale bars: 2 mm (**A**); 20 μm (**E**). $^{**}P < 0.01$.

control mouse IMCD3 cells transduced with the respective control siLuc or pGIPZ-NS lentivectors. Phospho-Rb was also increased in *Pkd1*-null MEK cells and PN24 cells, as well as in kidney tissues from *Pkd1*$^{nl/nl}$ mice, compared with that seen in the respective WT MEK cells, PH2 cells, and control kidney tissues (Figure 8, B and C).

To support the functional relationship between SIRT1 and Rb in renal epithelial cells, we found that SIRT1 interacted with Rb by demonstrating that anti-Rb antibody could pull down SIRT1 (Figure 8D). Due to the lack of antibodies for acetyl-Rb, we used anti-Rb antibody to pull down Rb and subsequently used an anti–acetyl-α-lysine antibody to evaluate the acetylation of Rb, as performed by other laboratories (24, 25). We found that acetylated Rb was decreased in SIRT1 upregulating *Pkd1*-null MEK versus WT MEK cells (Figure 8D). In addition, we found that (a) overexpressing WT SIRT1, but not SIRT1-H355A, decreased the acetylation level of Rb and increased the level of phospho-Rb in mouse IMCD3 cells (Figure 9, A and B); (b) silencing SIRT1 with siRNA or inhibiting SIRT1 activity with nicotinamide increased the acetylation level of Rb in *Pkd1*-null MEK cells compared with appropriate controls (Figure 9, C and D); and (c) silencing SIRT1 with siRNA or inhibiting SIRT1 activity with nicotinamide decreased phospho-Rb levels in *Pkd1*-null MEK cells and PN24 cells compared with untreated control cells (Figure 9, E and F). Rb regulates the cell cycle through its interaction with the E2F family of transcription factors, in that Rb dephosphorylation increases Rb-E2F1 complex formation, and Rb phosphorylation releases E2F1 from Rb–E2F complexes, enabling E2F-dependent transcription of genes that mediate S-phase entry (26, 27). We found that the expression of E2F1 downstream targets DHFR, cyclin D3, and cyclin E, which are involved in cell cycle regulation, was upregulated in PN24 cells compared with PH2 cells, while levels of these proteins decreased in nicotinamide-treated versus untreated PN24 cells (Supplemental Figure 7). These results suggested that SIRT1 regulates renal cystic epithelial cell proliferation through Rb-E2F1 signaling.

Nicotinamide induces cystic epithelial cell death through p53-mediated cell death pathway. Treatment with nicotinamide increased cystic epithelial cell death in *Pkd1*-knockout renal tissues. Previous studies demonstrated that SIRT1 protects cells from p53-mediated apoptosis through a deacetylation-dependent mechanism (10, 28, 29). Thus, we examined whether SIRT1-mediated p53 deacetylation was involved in nicotinamide-induced cystic epithelial cell death. We found that (a) SIRT1 interacted with p53 by demonstrating that anti-p53 antibody could pull down endogenous SIRT1 and that anti-SIRT1 antibody could pull down endogenous p53 in WT MEK cells and *Pkd1*-null MEK cells (Figure 10A); (b) p53 acetylation was decreased in *Pkd1*-null MEK cells versus WT MEK cells, while p53 expression exhibited no difference between these cells (Figure 10B); (c) overexpressing HA-tagged WT SIRT1, but not SIRT1-H355A, in mouse IMCD3 cells decreased p53 acetylation, but had no effect

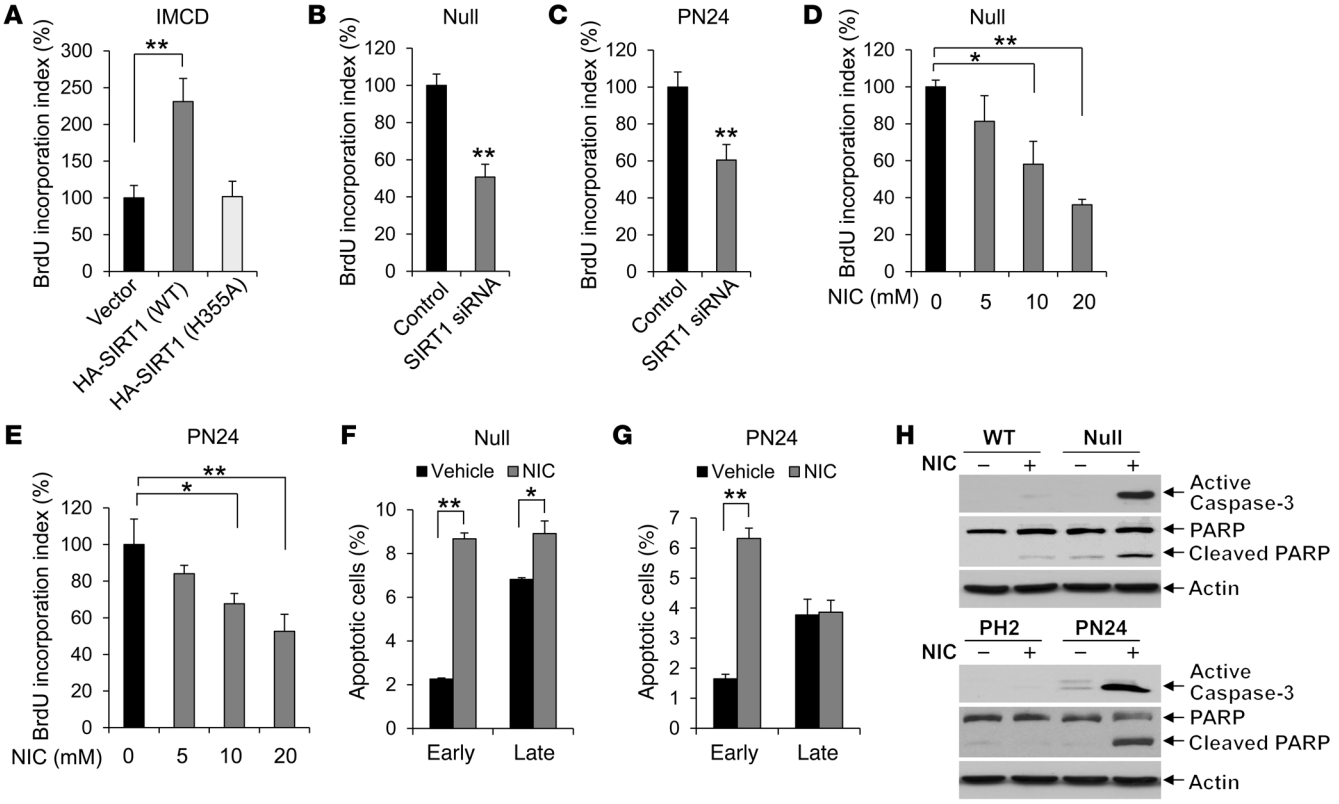

Figure 7

Silence or inhibition of SIRT1 decreased renal epithelial cell proliferation, but increased apoptosis. (**A**) Overexpressing WT SIRT1, but not deacetylase catalytically inactive mutant SIRT1 H355A, increased BrdU incorporation in mouse IMCD3 cells compared with cells transfected with vector alone. (**B**–**E**) Silencing SIRT1 with siRNA (**B** and **C**) or inhibiting SIRT1 with the indicated concentrations of nicotinamide (**D** and **E**) decreased BrdU incorporation in (**B** and **D**) *Pkd1*-null MEK and (**C** and **E**) PN24 cells. BrdU incorporation index in the control cells was assigned as 100%. An average of 300 cells was counted for each experiment. $n = 3$. (**F** and **G**) Flow cytometry analysis indicated that apoptosis was induced in (**F**) *Pkd1*-null MEK cells treated with 10 mM nicotinamide for 24 hours and (**G**) PN24 cells treated with 40 mM nicotinamide for 48 hours. Nicotinamide-treated cells were labeled with annexin V and PI and analyzed by flow cytometry. Early and late apoptotic cells were represented by annexin V^+PI^- and annexin V^+PI^+ cells, respectively. $n = 3$. (**H**) Caspase-3 activation was examined from whole cell lysates of WT MEK, *Pkd1*-null MEK, PH2, and PN24 cells treated or not with 10 mM nicotinamide for 24 hours. Nicotinamide treatment increased caspase-3 activation and caused the appearance of cleaved PARP (a substrate of caspase-3) in *Pkd1*-null MEK and PN24 cells. $^*P < 0.05$; $^{**}P < 0.01$.

on p53 expression (Supplemental Figure 8); (d) silencing SIRT1 with siRNA or inhibiting SIRT1 activity with its inhibitor, nicotinamide, increased the level of acetyl-p53 but had no effect on p53 expression in *Pkd1*-null MEK cells and PN24 cells compared with untreated control cells (Figure 10, C and D); (e) knockdown of p53 with siRNA prevented nicotinamide-induced caspase-3 activation and cystic epithelial cell death in *Pkd1*-null MEK cells and PN24 cells (Figure 11, A and B, and Supplemental Figure 9, A and B); and (f) overexpression of WT p53, but not mutant p53-8KR (which is mutated at 8 acetylation sites; ref. 30), increased apoptosis in *Pkd1*-null MEK cells treated with nicotinamide (Figure 11C). These results suggested that SIRT1 mediates p53 deacetylation involved in nicotinamide-induced cell death in *Pkd1*-mutant epithelia.

Discussion

This study demonstrated a novel functional role of SIRT1 in ADPKD and provided a molecular basis for using nicotinamide (vitamin B3) to delay cyst formation. We found that SIRT1 expression was increased in *Pkd1*-mutant renal epithelial cells and tissues. Genetic deletion of *Sirt1* in *Pkd1*–conditional knockout mice delayed renal cyst formation in postnatal kidneys. Inhibiting SIRT1 with nicotinamide (14) or the SIRT1-specific inhibitor EX-527 (21) delayed cyst formation in *Pkd1*-null MEKs, in *Pkd1*–conditional knockout postnatal kidneys, and in hypomorphic $Pkd1^{nl/nl}$ mouse kidneys, establishing an in vivo connection between SIRT1 and loss of PC1-mediated cyst formation (Figure 11D). In addition, we provided evidence that PC1 affects SIRT1 expression in renal epithelial cells through c-MYC. We conclude that increased SIRT1 in *Pkd1*-mutant renal epithelial cells (a) is a target of nicotinamide, which decreases proliferation and induces apoptosis of cystic epithelial cells; (b) regulates cystic epithelial cell proliferation through decreasing the acetylation and increasing the phosphorylation of Rb to regulate Rb-E2F1–mediated S-phase entry; (c) regulates p53 acetylation and p53-dependent apoptosis in response to nicotinamide; and (d) is regulated by c-MYC and can be further induced by TNF-α, which is present in cyst fluid during cyst development (Figure 11D). Since nicotinamide is a B3 vitamin with little toxicity reported, it has great therapeutic potential in ADPKD treatment.

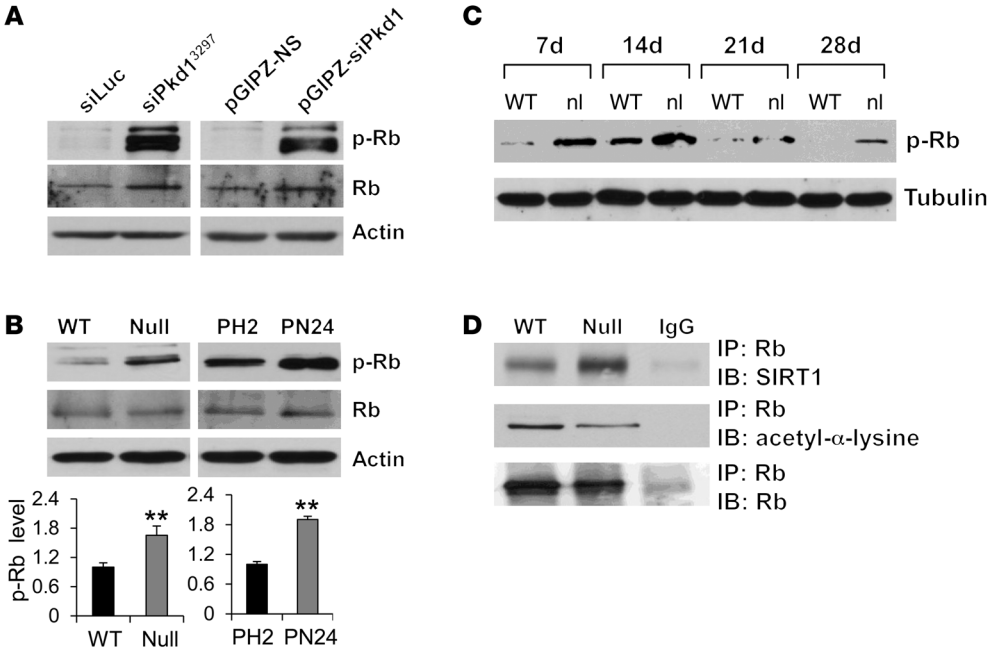

Figure 8

SIRT1 interacts with Rb. (**A** and **B**) Western blot analysis of Rb and phospho-Rb expression (**A**) in mouse IMCD3 cells with *Pkd1* knockdown by 2 different lentivirus-mediated *Pkd1* shRNAs (as in Figure 1C) and (**B**) from whole cell lysates of WT MEK, *Pkd1*-null MEK, PH2, and PN24 cells. In **B**, relative phospho-Rb level (standardized to actin) from 3 independent immunoblots is also shown. (**C**) Western blot analysis of phospho-Rb expression in kidneys from WT and $Pkd1^{nl/nl}$ mice collected at P7, P14, P21, and P28. (**D**) Interaction between SIRT1 and Rb and levels of acetyl-Rb in WT MEK and *Pkd1*-null MEK cells, examined by IP with anti-Rb antibody and then blotting with SIRT1 antibody and anti–acetyl-α-lysine antibody. IgG was used as a negative control. $^{**}P < 0.01$.

SIRT1 is expressed abundantly in renal medullary interstitial cells, but at low levels in the renal cortex (31), which suggests that only low levels of SIRT1 may be detected in normal kidney epithelial cells. In the present study, we found that SIRT1 expression was markedly increased in DBA-positive *Pkd1*-null MEK cells and *Pkd1*-mutant postnatal proximal tubular–derived PN24 cells as well as in *Pkd1*-knockdown mouse IMCD3 cells and cyst lining epithelia of *Pkd1*-knockout kidney tissues (Figure 1). Our in vivo results demonstrating that cyst development was significantly delayed in ADPKD mice with a *Sirt1*-null background (Figure 3) strongly support an in vivo function of SIRT1 in ADPKD. A recent study reports that kidney-specific SIRT1 overexpression in proximal tubules does not appear to make mice susceptible to kidney cysts, but instead is protective against the consequence of ischemic and obstructive injury. These data suggest that overexpression of SIRT1 in proximal tubules, in the presence of WT PC1, may not result in renal cyst formation (32). Thus, the most plausible explanation for a pathological role of SIRT1 in renal cystogenesis is that PC1 mutations fundamentally change renal epithelial cells essential for cyst formation, and this process is modulated by SIRT1 activity.

Nicotinamide is a known inhibitor of SIRT1, and nicotinamide alters SIRT1-mediated downstream signaling pathways (14, 33). However, nicotinamide may inhibit the activity of other sirtuin proteins, including SIRT2–SIRT4 (14, 34, 35). To address the concern that nicotinamide might be targeting other sirtuin family members to delay renal cyst growth, we conducted several experiments and found that (a) in vivo administration of nicotinamide did not provide an added benefit in $Pkd1^{flox/flox}$:$Sirt1^{flox/flox}$:*Ksp-Cre* double-knockout mice (Supplemental Figure 4, B–D), and (b) administration of nicotinamide or EX-527 had similar effects on delaying cyst growth in *Pkd1*-knockout mouse models (Figures 5 and 6). We also found that knockdown of SIRT1 with siRNA and inhibition of SIRT1 with nicotinamide had similar effects on SIRT1-mediated Rb phosphorylation and p53 deacetylation in vitro. Thus, we attribute the effects of nicotinamide on delaying cyst formation to its inhibition of SIRT1-mediated signaling pathways in cystic epithelial cells.

We focused on nicotinamide due to the relative safety of its administration even at high doses for a variety of therapeutic applications (36). Our findings that nicotinamide delayed cyst growth not only in an aggressive $Pkd1^{flox/flox}$:*Ksp-Cre* mouse model (Figure 5), but also in $Pkd1^{nl/nl}$ mice (Figure 6), a progressive hypomorphic mouse model that has been recognized to closely resemble human ADPKD, support the potential clinical utility of nicotinamide in ADPKD patients. It has been reported that a 3-g/d dosage of nicotinamide is safe for adults (36). The dosage and route of administration of nicotinamide for treating ADPKD patients merits further investigation.

Increased proliferation is a crucial component of cystic expansion in ADPKD. There are several different signaling pathways that have been reported to regulate cystic epithelial cell proliferation (37, 38). In this study, we provided evidence that SIRT1-mediated deacetylation and phosphorylation of Rb, which inactivates Rb, regulated cystic epithelial cell proliferation (Figures 8 and 9). Rb is a central cell cycle regulator whose functions are in part regulated by diverse means, including posttranslational modifications such as phosphorylation and acetylation (12, 24). Active Rb is hypophosphorylated, and inactive Rb is hyperphosphorylated. Active Rb functions

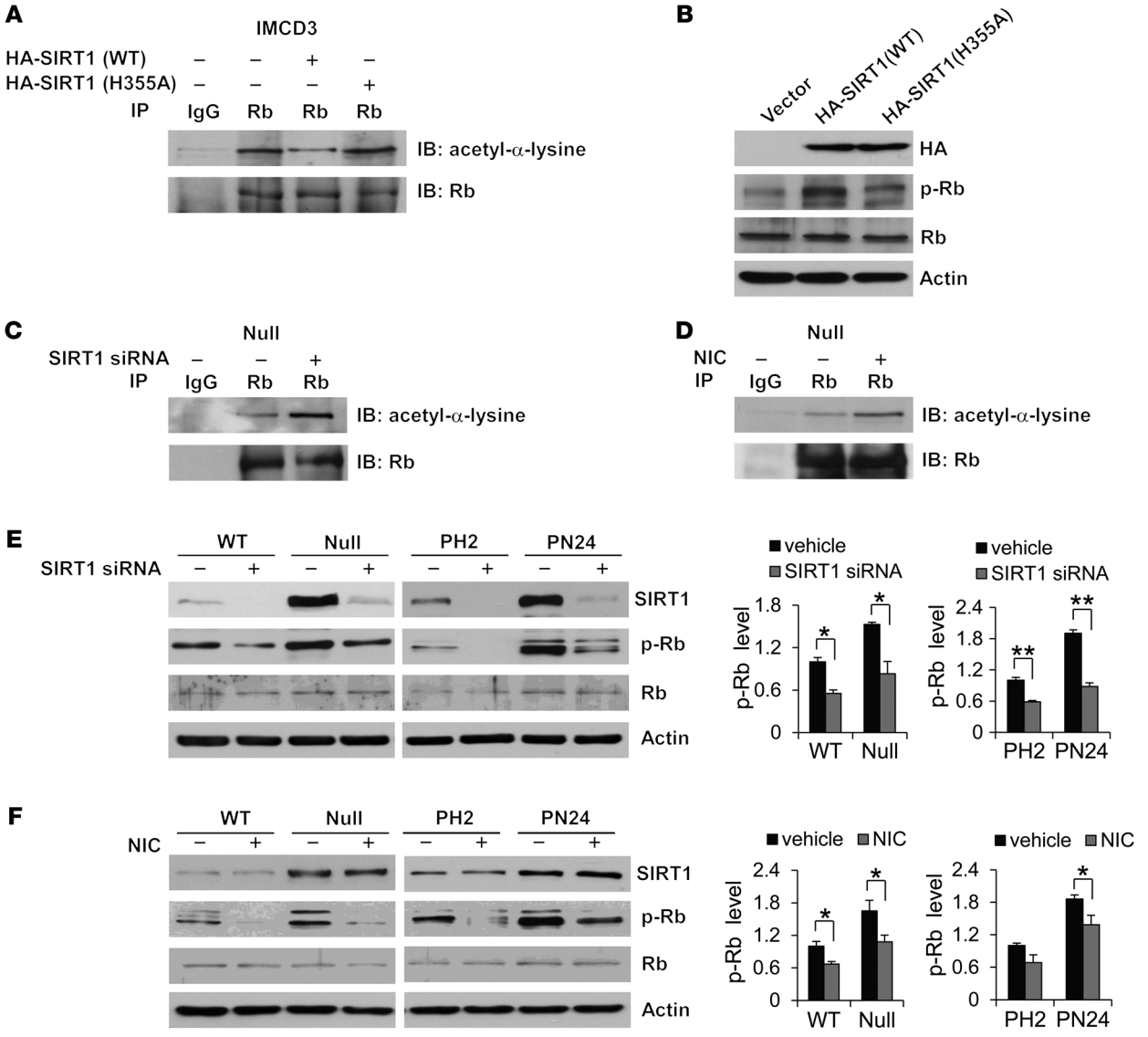

Figure 9

Interaction of SIRT1 with Rb mediates Rb deacetylation and phosphorylation. (**A** and **B**) Overexpression of WT SIRT1, but not deacetylase catalytically inactive mutant SIRT1 H355A, (**A**) decreased the level of acetylated Rb, as examined with anti–acetyl-α-lysine antibody after Rb was pulled down with anti-Rb antibody, and (**B**) increased the level of phospho-Rb, as examined by Western blot, in mouse IMCD3 cells transfected with WT SIRT1, mutant SIRT1 H355A, or empty vector for 48 hours. (**C** and **D**) Knockdown of SIRT1 with siRNA or inhibition of SIRT1 with nicotinamide increased the acetylation level of Rb in *Pkd1*-null MEK cells that were (**C**) transfected with SIRT1 siRNA for 48 hours or (**D**) treated with 10 mM nicotinamide for 24 hours. Rb acetylation was analyzed as above. (**E** and **F**) Knockdown of SIRT1 with siRNA or inhibition of SIRT1 with nicotinamide decreased Rb phosphorylation, but did not affect Rb expression, in WT MEK, *Pkd1*-null MEK, PH2, and PN24 cells that were (**E**) transfected with SIRT1 siRNA for 48 hours or (**F**) treated with 10 mM nicotinamide for 24 hours. *$P < 0.05$; **$P < 0.01$.

to repress the cell cycle through its interaction with the E2F family of transcription factors (26) and recruitment of chromatin-remodeling enzymes, such as histone deacetylases (HDACs), components of SWI2/SNF2 complex and methyltransferases, to E2F target gene promoters containing E2F sites (39, 40). However, phosphorylation of Rb can reverse this repression through dissociation of Rb–E2F complexes, enabling E2F-dependent transcription of genes that mediate S-phase entry (27). We found that SIRT1 regulated the acetylation and phosphorylation of Rb, since knockdown of SIRT1 with siRNA or inhibition of SIRT1 activity with nicotinamide increased Rb acetylation and decreased Rb phosphorylation (Figures 8 and 9). Treatment with nicotinamide also decreased the expression of the E2F1 targets DHFR, cyclin D3, and cyclin E, which were upregulated in *Pkd1*-mutant renal epithelial cells (Supplemental Figure 7). These data suggest that SIRT1 regulates (in part) cystic epithelial cell proliferation by altering the phosphorylation status of Rb and most likely through a Rb-mediated E2F pathway.

Increased levels of apoptosis are observed in human ADPKD as well as in rodent models of ADPKD and autosomal-recessive polycystic kidney disease (ARPKD) (41). However, apoptotic cells

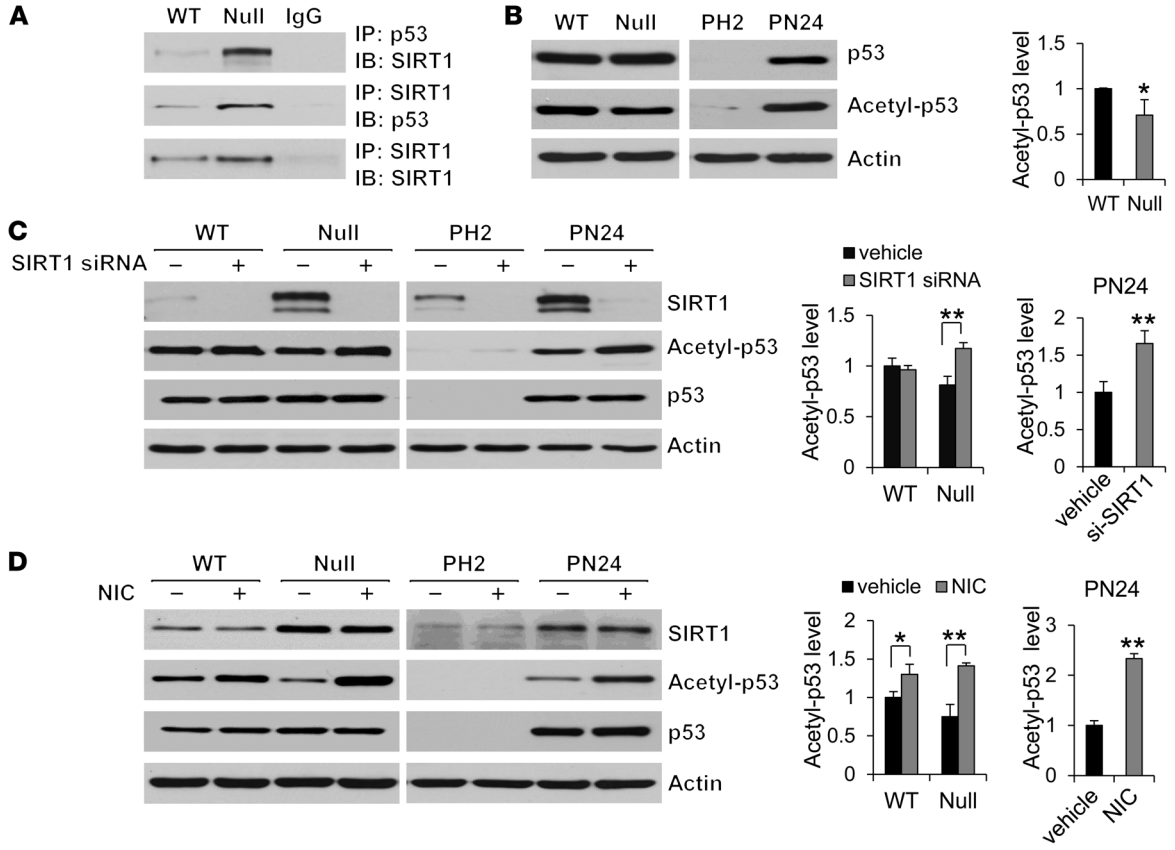

Figure 10

SIRT1 interacts and deacetylates p53 in renal epithelial cells. (**A**) The interaction between SIRT1 and p53 in WT and *Pkd1*-null MEK cells was examined by co-IP using either anti-SIRT1 or anti-p53 antibody. IgG was used as a negative control. (**B**) Western blot analysis of p53 and acetyl-p53 expression from whole cell lysates of WT MEK, *Pkd1*-null MEK, PH2, and PN24 cells. Acetyl-p53 expression was decreased in *Pkd1*-null MEK versus WT MEK cells, whereas p53 expression was almost at same levels in these cells. (**C** and **D**) Knockdown of SIRT1 with siRNA or inhibition of SIRT1 with nicotinamide increased p53 acetylation, but did not affect p53 expression, in *Pkd1*-null MEK cells and PN24 cells that were (**C**) transfected with SIRT1 siRNA for 48 hours or (**D**) treated with 10 mM nicotinamide for 24 hours. $^{*}P < 0.05$, $^{**}P < 0.01$.

were rare in kidneys from models of conventional and conditional *Pkd1* knockout (Figures 4–6), consistent with previous findings that the overall number of apoptotic nuclei in *Pkd1*$^{flox/-}$*:Ksp-Cre* or *Pkd2-WS25* mouse kidneys is very low and is not significantly different between cystic and normal kidneys (42, 43). These observations are in contrast with the proposed role of apoptosis in mediating progressive loss of normal renal tissue during cyst development in a *Pkd1* mutant mouse model. In this study, we provide evidence that SIRT1-mediated p53 deacetylation, which inactivates p53, may survive cystic epithelial cells from p53-mediated apoptosis during cyst development. We found that treatment with nicotinamide not only induced cystic epithelial cell apoptosis (Figure 7), but also increased p53 acetylation (Figure 10). Knockdown of p53 with siRNA in *Pkd1*-mutant cells blocked nicotinamide-induced cell death (Figure 11, A and B, and Supplemental Figure 9, A and B), which further supports the involvement of p53 in regulating cystic epithelial cell apoptosis. However, nicotinamide may also induce cystic epithelial cell apoptosis through other SIRT1-mediated pathways, such as FOXO3α and E2F1. Prior reports demonstrate that SIRT1 inhibits oxidative stress–induced apoptosis through FOXO3α activation and catalase upregulation in HK-2 cells (44). In addition, E2F1, which is stabilized and activated by DNA damage, stimulates the transcription of several genes in the apoptotic pathways (11). Whether FOXO3α and E2F1 are involved in nicotinamide-induced cystic epithelial cell death needs further investigation.

In addition, our present findings support a regulatory role for c-MYC and TNF-α on SIRT1 expression in *Pkd1*-mutant renal epithelial cells (Figure 2). Mutations of *Pkd1* increase c-MYC expression, which as an initiating event increases SIRT1 expression. During cyst development, TNF-α is secreted into cyst fluid via an uncertain mechanism, which as a secondary event further stimulates the expression of SIRT1 through TNF-α–mediated NF-κB activation. SIRT1 has been shown to suppress NF-κB activity through deacetylating p65 in different cell lines, which inhibits the inflammation induced by NF-κB (45–47). Whether there is a feedback loop between SIRT1 expression and NF-κB activation in cystic epithelial cells and whether TNF-α signaling is able to override the inhibition of SIRT1 on NF-κB will require further investigation.

In sum, our present study identified SIRT1 as a novel regulator of cyst formation and provided the molecular mechanism and rationale for using nicotinamide (vitamin B3) as a novel therapeutic intervention in ADPKD to delay cyst formation. Our results that

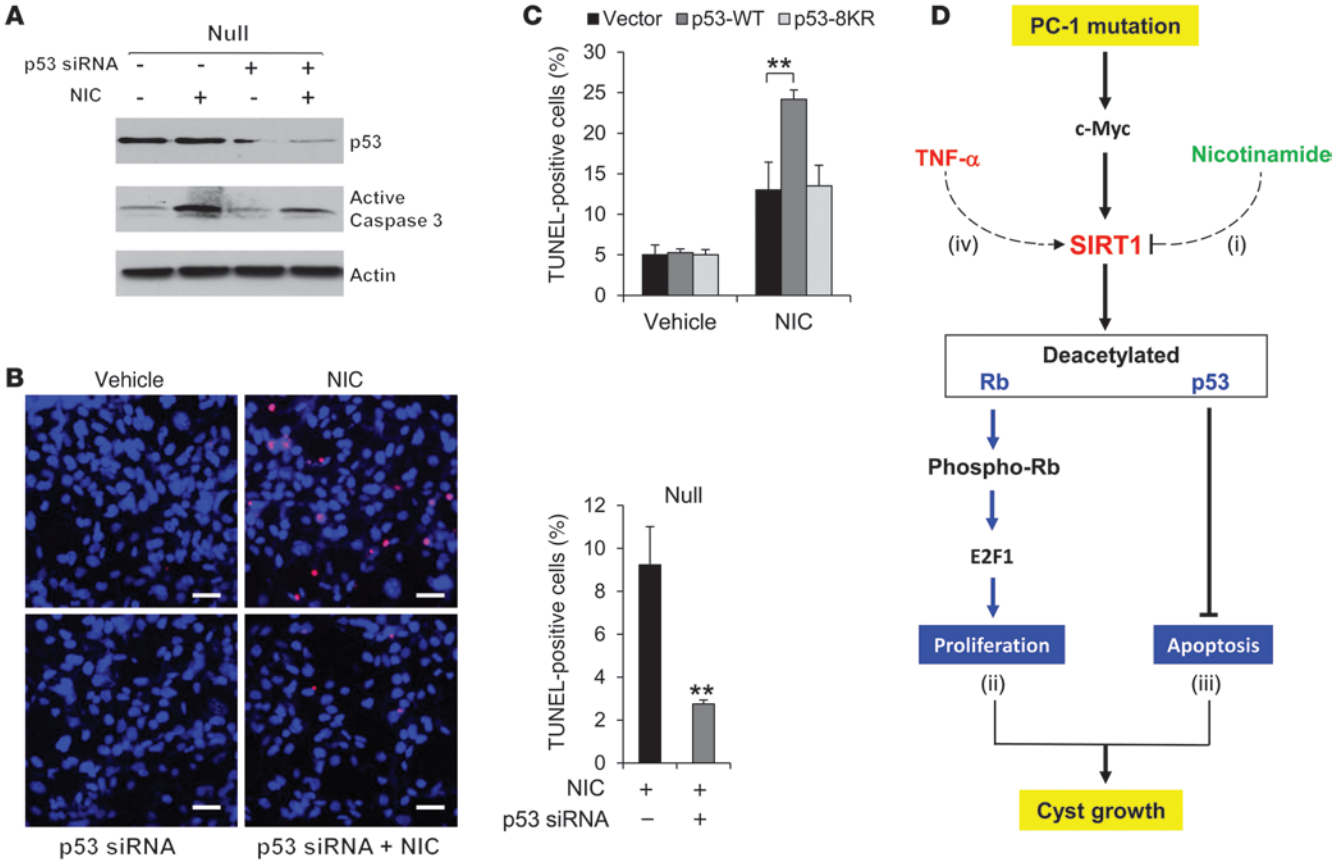

Figure 11

Nicotinamide induces cystic epithelial cell death through p53. (**A**) Western blot analysis of p53 and active caspase-3 expression in *Pkd1*-null MEK cells transfected or not with p53 siRNA for 24 hours and then treated or not with 10 mM nicotinamide for another 24 hours. (**B**) Knockdown of p53 with siRNA prevented nicotinamide-induced apoptosis, as detected by TUNEL assay, in *Pkd1*-null MEK cells that were transfected or not with p53 siRNA for 24 hours and then treated or not with 10 mM nicotinamide for 24 hours. (**C**) Overexpression of WT p53, but not mutant p53-8KR (which is mutated at 8 acetylation sites), increased apoptosis in *Pkd1*-null MEK cells treated with nicotinamide. *Pkd1*-null MEK cells were transfected with WT p53, mutant p53-8KR, or empty vector together with or without nicotinamide for 24 hours, then analyzed by TUNEL assay. (**D**) SIRT1-mediated pathways in *Pkd1*-mutant renal epithelial cells. *Pkd1* knockout or mutation upregulates SIRT1 through c-MYC. Upregulated SIRT1 in *Pkd1*-mutant renal epithelial cells (i) is a target of nicotinamide, which decreases proliferation and induces apoptosis of cystic epithelial cells to delay cyst growth in *Pkd1*-null mouse kidneys; (ii) regulates the acetylation and phosphorylation of Rb and further affects Rb-E2F–mediated S-phase entry; (iii) regulates the p53 acetylation and p53-dependent apoptosis in response to nicotinamide; and (iv) can be regulated by c-MYC and induced by TNF-α. Scale bars: 50 μm. $^{**}P < 0.01$.

nicotinamide delayed cyst formation in MEKs when administered to pregnant females (Figure 4) suggest the possibility that at-risk fetuses, based on family history, may be treated in utero by administration of nicotinamide to the pregnant mother. In addition, since nicotinamide delayed cyst growth in postnatal *Pkd1*-knockout mouse kidneys (Figures 5 and 6), administration of nicotinamide to a neonate, toddler, or adolescent may delay cyst growth.

Methods

Cell culture and reagents. Murine IMCD3 cells and HEK-293T cells were maintained at 37°C in 5% CO_2 in DMEM (Invitrogen) supplemented with 10% FBS. WT and *Pkd1*-null MEK cells, derived from collecting ducts and sorted by the collecting duct marker dolichos biflorus agglutinin (DBA) from kidneys of WT and *Pkd1*-null mice (48), were maintained as previously described (38). PH2 and PN24 cells (provided by S. Somlo through the George M O'Brien Kidney Center, Yale University, New Haven, Connecticut, USA) were cultured as described previously (42). Primary human ADPKD and NHK cells (provided by D. Wallace, University of Kansas Medical Center, Kansas City, Kansas, USA) were cultured as described previously (19). Nicotinamide, TNF-α, and EX-527 were purchased from Sigma-Aldrich. SN50 was purchased from EMD Millipore.

pCruZ-HA-SIRT1 (WT SIRT) and pcDNA3-c-MYC plasmids were purchased from Addgene (49). pCruz-HA-SIRT1 (SIRT-H355A) was constructed using a Site Directed Mutagenesis Kit (Stratagene). For overexpression of WT SIRT1, mutant SIRT1-H355A, or c-MYC, constructs were transfected into mouse IMCD3 cells, WT MEK cells, or PH2 cells, respectively. After transfection for 48 hours, cells were harvested and analyzed by Western blot.

pCin4-p53 (WT) and pCin4-p53-8KR (8 acetylation sites mutant p53) plasmids were provided by W. Gu (Columbia University, New York, New York, USA). *Pkd1*-null MEK cells were transfected with pCin4-p53, pCin4-p53-8KR, or empty vector, either with or without nicotinamide treatment. After transfection for 24 hours, cells were analyzed by TUNEL assay.

IP and Western blot. We performed IP and Western blotting on whole-cell lysates as previous described (38). Briefly, cells were lysed at 4°C with modified lysis buffer consisting of 20 mM Tris-HCl (pH 7.5), 1% Triton X-100, 150 mM NaCl, 1% glycerol, 0.5 mM dithiothreitol, and 1 mM sodium vanadate plus protease inhibitor (Roche Applied Science). Cell extracts were clarified by centrifuging at 16,000 *g* for 15 minutes at 4°C, and the supernatants were subjected to IP with anti-SIRT1 (Cell Signaling Technologies), anti-Rb (Santa Cruz), or anti-p53 (Cell Signaling Technologies) antibodies. After incubation at 4°C overnight, protein A agarose beads were added and incubated at 4°C for another 2 hours. Immunocomplexes were then subjected to Western blot analysis.

The antibodies used for Western analysis included anti-SIRT1, anti–phospho-Rb, anti–acetyl-α-lysine, anti-p53, anti–acetyl-p53, anti-PARP, and anti-active caspase-3 antibodies (Cell Signaling Technologies; 1:1,000 dilution); anti-actin and anti-tubulin antibodies (Sigma-Aldrich; 1:5,000 dilution); and anti-Rb, anti-HA, anti-DHFR, anti–cyclin E, anti–c-MYC, and anti–cyclin D3 antibodies (Santa Cruz; 1:500 dilution). All primary antibodies were used at 1:50 dilution for IP and as indicated above for Western blotting. Donkey anti-rabbit IgG–horseradish peroxidase and donkey anti-mouse IgG–horseradish peroxidase (Santa Cruz; 1:8,000 dilution) were used as secondary antibodies.

Immunohistochemistry. Kidneys were fixed with 4% paraformaldehyde (pH 7.4). For PCNA staining, a monoclonal mouse anti-PCNA antibody (Cell Signaling Technologies; 1:1,000 dilution), a biotinylated secondary antibody (Sigma-Aldrich; 1:100 dilution), and DAB substrate system were used. For SIRT1 staining, a rabbit anti-SIRT1 antibody (Cell Signaling Technologies; 1:100 dilution) and a rabbit anti-hSIRT1 antibody (Epitomics; 1:100 dilution) were used. Kidney sections were counterstained by hematoxylin. Images were analyzed with a NIKON ECLIPSE 80i microscope.

Pkd1 knockdown by lentivirus carrying Pkd1 shRNA. HEK293T cells were transfected either with lentiviral plasmid pGIPZ-siPkd1 (Open Biosystems), carrying *Pkd1* shRNA, or with control empty vector pGIPZ-NS, plus psPAX2 packaging plasmid and pMD2.G envelope plasmid using calcium phosphate. After transfection for 12 hours, the medium containing the transfection reagent was removed and replaced with fresh complete DMEM plus 10% FBS and penicillin/streptomycin. The lentiviral particles were harvested from HEK293T cells after another 48 hours. Mouse IMCD3 cells were then infected with appropriate amounts of lentiviral particles together with 5 μg/ml polybrene (Sigma-Aldrich) for 24 hours, and then virus-containing medium was removed and replaced with fresh medium plus 10 μg/ml puromycin. After 48 hours of puromycin selection, all remaining cells were GFP positive, as detected by microscopy. Mouse IMCD3 cells were harvested after lentiviral particle infection for 5 days and analyzed by RT-PCR to examine the efficiency of *Pkd1* knockdown. We also used another lentiviral plasmid, VIRHD/P/siPkd1^{3297} (carrying *Pkd1* shRNA), to knock down *Pkd1* in mouse IMCD3 cells with the same protocol described above; the empty vector, VIRHD/P/siLuc, was used as control (both provided by G.L. Gusella, Mount Sinai School of Medicine, New York, New York, USA; ref. 50).

qRT-PCR. Total RNA was extracted using the RNeasy plus mini kit (Qiagen). 1 μg total RNA was used for RT reactions in a 20-μl reaction to synthesize cDNA using Iscript cDNA Synthesis Kit (BioRad). RNA expression profiles were analyzed by real-time PCR using iTaq SYBER Green Supermix with ROX (BioRad) in an icycler iQTM Real-time PCR detection system. Genes were amplified using the following primers: PKD1 forward, 5′-TCAATTGCTCCGGCCGCTG-3′; PKD1 reverse, 5′-CCAGCGTCTGAAGTAGGTTGTGGG-3′; SIRT1 forward, 5′-CTCTGAAAGTGAGACCAGTAG-3′; SIRT1 reverse, 5′-TGTAGATGAGGCAAAGGTTCC-3′; actin forward, 5′-AAGAGCTATGAGCTGCCTGA-3′; actin reverse, 5′-TACGGATGTCAACGTCACAC-3′. The complete reactions were subjected to the following program of thermal cycling: 40 cycles of 10 seconds at 95°C and 20 seconds at 63°C. A melting curve was run after the PCR cycles, followed by a cooling step. Each sample was run in triplicate in each experiment, and each experiment was repeated 3 times. Expression levels of PKD1 and SIRT1 were normalized to the expression level of actin.

RNA interference. The RNA oligonucleotides that specifically targeted mouse SIRT1, mouse c-MYC, and mouse p53 were purchased from Thermo Dharmacon. The RNA oligonucleotides were transfected with DharmaFECT siRNA transfection reagent (Dharmacon). 48 hours after transfection, cells were harvested and analyzed by Western blotting.

ChIP assay. ChIP assay was performed according to the manufacturer's protocol (EZ CHIP Chromatin Immunoprecipitation Kit; Upstate Biotechnology). Chromatin DNA was subjected to IP with anti–c-MYC antibody (SC-764; Santa Cruz) or normal rabbit IgG and then washed, after which the DNA-protein cross-links were reversed. The recovered DNA was analyzed by PCR for the presence of c-MYC binding motifs at mouse SIRT1 promoter between –1,009 and –850 bp (E1) and between –2,535 and –2,385 bp (E2) upstream of the SIRT1 ATG start codon. The PCR amplification for distant regions (–3,178 to –3,023 bp) was used as a negative control. The primers for E1 are 5′-AGACAGGGAGGGATGGATG-3′ and 5′-AGCCTGGCTATGTCCACAAT-3′; the primers for E2 are 5′-CCTCACTGCTCCCACAGAG-3′ and 5′-TCCGTGGAAGTGTACCTTGG-3′. A pair of distant primers (5′-AATTTTCACCACCCCTCCTC-3′ and 5′-GACAGAGGCAGGTGGATCTC-3′) was used as negative control.

TUNEL assay. TUNEL assay for nicotinamide-treated WT MEK, *Pkd1*-null MEK, PH2, and PN24 cells and for nicotinamide- or EX-527–treated kidneys was performed according to the manufacturer's protocols (In Situ Death Detection Kit; Roche). Prolong Gold Anti-fade reagent with DAPI (Invitrogen) was used. Immunofluorescence images were obtained with a NIKON ECLIPSE 80i microscope.

Apoptosis assays. Apoptosis was measured by flow cytometry with the FITC Annexin-V Apoptois Detection Kit (BD Pharmingen) according to the manufacturer's instruction. Annexin V$^+$PI$^-$ and annexin V$^+$PI$^+$ cells were considered early and late apoptotic cells, respectively.

BrdU incorporation assay. For BrdU incorporation assay in cells transfected with WT SIRT1 plasmid, SIRT1-H355A plasmid, or SIRT1 siRNA, after 12 hours of transfection, cells were induced to growth arrest by serum starvation for 24 hours, then cultured in regular media for another 12 hours. Subsequently, cells were pulse labeled with 10 μM BrdU for 1 hour, followed by a 12-hour chase, and then stained by anti-BrdU antibody (Sigma-Aldrich; 1:1,000 dilution). For BrdU incorporation assay in nicotinamide-treated cells, the cells were cultured with 5, 10, or 20 mM nicotinamide for 24 hours, then treated as described above. The percentage of BrdU-positive cells was counted; BrdU incorporation indices are shown relative to the control value (assigned as 100%).

Mouse strains and treatment. *Pkd1*$^{null/+}$ mice, generated as described previously (51), were used to examine the effect of nicotinamide on cyst growth during embryogenesis. In brief, *Pkd1*-heterozygous mice (51) were paired, and pregnant females were injected i.p. daily, from 7.5 dpc to 14.5 or 17.5 dpc, with nicotinamide (0.5 mg/g body weight) or an equal volume of the vehicle DMSO. At the end of treatment, females were sacrificed, and MEKs were collected and fixed in 4% paraformaldehyde. Genomic DNA from the embryos was obtained (XNAT Extract-N-Amp Tissue PCR Kit; Sigma-Aldrich) and genotyped (JumpStart Kit; Sigma-Aldrich).

Pkd1$^{flox/flox}$*:Ksp-Cre* mice were used to test the effect of nicotinamide or EX-527 on cyst progression at P7. *Pkd1*$^{flox/flox}$ mice and *Ksp-Cre* transgenic mice were generated as described previously (42, 52). *Pkd1*$^{flox/flox}$ mice (B6; 129S4-*Pkd1*^{tm2Ggg}/J; stock 010671; Jackson Laboratories) possess loxP sites on either side of exons 2–4 of *Pkd1* (42). *Ksp-Cre* mice express Cre recombinase under the control of the Ksp-cadherin promoter (52). *Pkd1*$^{flox/flox}$*:Ksp-Cre* mice

were generated by cross-breeding *Pkd1*$^{flox/flox}$ female mice with *Pkd1*$^{flox/+}$*:Ksp-Cre* male mice. Each neonate was injected i.p. daily with 0.25 mg/g nicotinamide, 2 mg/kg EX-527, or DMSO from P3 to P6. All kidneys from 5 female mice and 5 male mice per group were harvested and analyzed at P7.

Sirt1$^{flox/flox}$ mice (B6; 129-*Sirt1*^{tm1Ygu}/J; stock 008041; Jackson Laboratories), which possess loxP sites upstream and downstream of exon 4 of *Sirt1*, were used to generated the *Sirt1* and *Pkd1* double-knockout mice. First, we generated *Pkd1*$^{flox/+}$*:Sirt1*$^{flox/+}$*:Ksp-Cre* mice by crossing *Pkd1*$^{flox/+}$*:Ksp-Cre* mice with *Sirt1*$^{flox/flox}$ mice. Second, we generated *Pkd1*$^{flox/flox}$*:Sirt1*$^{flox/flox}$*:Ksp-Cre* mice by crossing *Pkd1*$^{flox/+}$*:Sirt1*$^{flox/+}$*:Ksp-Cre* female mice with *Pkd1*$^{flox/+}$*:Sirt1*$^{flox/+}$*:Ksp-Cre* male mice. We harvested kidneys and serum at P7 for further analysis. The *Pkd1*$^{flox/flox}$*:Sirt1*$^{flox/flox}$*:Ksp-Cre* neonates were also injected i.p. daily with 0.25 mg/g nicotinamide or DMSO from P3 to P6, and kidneys were harvested and analyzed at P7.

Hypomorphic *Pkd1*$^{nl/nl}$ mice, generated by cross-breeding *Pkd1*$^{nl/+}$ females with *Pkd1*$^{nl/+}$ males (15), were used to test the effect of nicotinamide or EX-527 on cyst progression at P28. Each neonate was injected i.p. daily with 0.25 mg/g nicotinamide, 2 mg/kg EX-527, or DMSO from P5 to P27, and the kidneys from 5 female mice and 5 male mice per group were harvested at P28 for further analysis.

The route of nicotinamide administration to animals was based on previous reports that nicotinamide could be administered to mice either by i.p. injection or via the drinking water at concentrations of 200–1,000 mg/kg (53–56). Compared with oral administration, i.p. injection is more efficient, and the amount of drug administered to animals is more controllable. Thus, we used i.p. injection of nicotinamide for treating *Pkd1*-knockout mouse models. Daily administration of nicotinamide was decided, given that (a) nicotinamide disappears rapidly from the circulation and is distributed in all tissues (57); (b) nicotinamide is readily absorbed parenterally and from all parts of the gastrointestinal tract (36); and (c) peak concentrations are achieved in humans within about 1 hour of oral ingestion of standard preparation (57). The time points of administration of nicotinamide to animals were based on studies using different drugs to treat *Pkd1*$^{flox/flox}$*:Ksp-Cre* mice (58) and prior observations of cyst development in *Pkd1*$^{nl/nl}$ mice (59).

Statistics. All data are presented as mean ± SEM. Unpaired 2-tailed Student's *t* test and χ^2 test were used to determine significance of differences. A *P* value less than 0.05 was considered significant.

Study approval. All animal protocols were approved and conducted in accordance with Laboratory Animal Resources of University of Kansas Medical Center and Institutional Animal Care and Use Committee regulations.

Acknowledgments

The authors are grateful for cell lines PH2 and PN24, provided by S. Somlo through the George M O'Brien Kidney Center at Yale University (NIH grant P30 DK079310). The authors also thank S. Parnel and P. Tran for helpful discussion and A. Artigues for technical support and discussion. X. Li acknowledges grant support from the PKD Foundation, Children's Research Institute, and the NIH (R01 DK084097). J.M. Denu acknowledges grant support from the NIH (R01 GM065386 and R01 GM059785), and E.D. Avner acknowledges grant support from the NIH (P50 DK079306; RCEPN).

Received for publication April 25, 2012, and accepted in revised form April 18, 2013.

Address correspondence to: Xiaogang Li, Department of Internal Medicine and the Kidney Institute, University of Kansas Medical Center, Mail Stop 3018, 3901 Rainbow Blvd., Kansas City, Kansas 66160, USA. Phone: 913.588.2731; Fax: 913.588.9251; E-mail: xli3@kumc.edu.

1. Harris PC. Autosomal dominant polycystic kidney disease: clues to pathogenesis. *Hum Mol Genet*. 1999;8(10):1861–1866.
2. Sweeney WE Jr, Avner ED. Diagnosis and management of childhood polycystic kidney disease. *Pediatr Nephrol*. 2011;26(5):675–692.
3. Torres VE, Harris PC. Mechanisms of Disease: autosomal dominant and recessive polycystic kidney diseases. *Nat Clin Pract Nephrol*. 2006;2(1):40–55.
4. Wu G, et al. Somatic inactivation of Pkd2 results in polycystic kidney disease. *Cell*. 1998;93(2):177–188.
5. Qian F, Watnick TJ, Onuchic LF, Germino GG. The molecular basis of focal cyst formation in human autosomal dominant polycystic kidney disease type I. *Cell*. 1996;87(6):979–987.
6. Li X. Epigenetics and autosomal dominant polycystic kidney disease. *Biochim Biophys Acta*. 2011;1812(10):1213–1218.
7. Guarente L. Franklin H. Epstein Lecture: Sirtuins, aging, and medicine. *N Engl J Med*. 2011; 364(23):2235–2244.
8. Finkel T, Deng CX, Mostoslavsky R. Recent progress in the biology and physiology of sirtuins. *Nature*. 2009;460(7255):587–591.
9. Kuzmichev A, et al. Composition and histone substrates of polycomb repressive group complexes change during cellular differentiation. *Proc Natl Acad Sci U S A*. 2005;102(6):1859–1864.
10. Luo J, et al. Negative control of p53 by Sir2alpha promotes cell survival under stress. *Cell*. 2001;107(2):137–148.
11. Wang C, et al. Interactions between E2F1 and SirT1 regulate apoptotic response to DNA damage. *Nat Cell Biol*. 2006;8(9):1025–1031.
12. Wong S, Weber JD. Deacetylation of the retinoblastoma tumour suppressor protein by SIRT1. *Biochem J*. 2007;407(3):451–460.
13. Michan S, Sinclair D. Sirtuins in mammals: insights into their biological function. *Biochem J*. 2007;404(1):1–13.
14. Avalos JL, Bever KM, Wolberger C. Mechanism of sirtuin inhibition by nicotinamide: altering the NAD(+) cosubstrate specificity of a Sir2 enzyme. *Mol Cell*. 2005;17(6):855–868.
15. Lantinga-van Leeuwen IS, et al. Lowering of Pkd1 expression is sufficient to cause polycystic kidney disease. *Hum Mol Genet*. 2004;13(24):3069–3077.
16. Lanoix J, D'Agati V, Szabolcs M, Trudel M. Dysregulation of cellular proliferation and apoptosis mediates human autosomal dominant polycystic kidney disease (ADPKD). *Oncogene*. 1996;13(6):1153–1160.
17. Yuan J, Minter-Dykhouse K, Lou Z. A c-Myc-SIRT1 feedback loop regulates cell growth and transformation. *J Cell Biol*. 2009;185(2):203–211.
18. Zeller KI, et al. Global mapping of c-Myc binding sites and target gene networks in human B cells. *Proc Natl Acad Sci U S A*. 2006;103(47):17834–17839.
19. Li X, et al. A tumor necrosis factor-alpha-mediated pathway promoting autosomal dominant polycystic kidney disease. *Nat Med*. 2008;14(8):863–868.
20. Zhang HN, et al. Involvement of the p65/RelA subunit of NF-kappaB in TNF-alpha-induced SIRT1 expression in vascular smooth muscle cells. *Biochem Biophys Res Commun*. 2010;397(3):569–575.
21. Solomon JM, et al. Inhibition of SIRT1 catalytic activity increases p53 acetylation but does not alter cell survival following DNA damage. *Mol Cell Biol*. 2006;26(1):28–38.
22. Leuenroth SJ, Bencivenga N, Igarashi P, Somlo S, Crews CM. Triptolide reduces cystogenesis in a model of ADPKD. *J Am Soc Nephrol*. 2008; 19(9):1659–1662.
23. Rodgers JT, Lerin C, Haas W, Gygi SP, Spiegelman BM, Puigserver P. Nutrient control of glucose homeostasis through a complex of PGC-1alpha and SIRT1. *Nature*. 2005;434(7029):113–118.
24. Chan HM, Krstic-Demonacos M, Smith L, Demonacos C, La Thangue NB. Acetylation control of the retinoblastoma tumour-suppressor protein. *Nat Cell Biol*. 2001;3(7):667–674.
25. Pickard A, Wong PP, McCance DJ. Acetylation of Rb by PCAF is required for nuclear localization and keratinocyte differentiation. *J Cell Sci*. 2010; 123(pt 21):3718–3726.
26. Dimova DK, Dyson NJ. The E2F transcriptional network: old acquaintances with new faces. *Oncogene*. 2005;24(17):2810–2826.
27. Dyson N. The regulation of E2F by pRB-family proteins. *Genes Dev*. 1998;12(15):2245–2262.
28. Vaziri H, et al. hSIR2(SIRT1) functions as an NAD-dependent p53 deacetylase. *Cell*. 2001;107(2):149–159.
29. Langley E, et al. Human SIR2 deacetylates p53 and antagonizes PML/p53-induced cellular senescence. *EMBO J*. 2002;21(10):2383–2396.
30. Tang Y, Zhao W, Chen Y, Zhao Y, Gu W. Acetylation is indispensable for p53 activation. *Cell*. 2008;133(4):612–626.
31. Hao CM, Haase VH. Sirtuins and their relevance to the kidney. *J Am Soc Nephrol*. 2010;21(10):1620–1627.
32. Hasegawa K, et al. Kidney-specific overexpression of Sirt1 protects against acute kidney injury by retaining peroxisome function. *J Biol Chem*. 2010;285(17):13045–13056.
33. Audrito V, et al. Nicotinamide blocks proliferation and induces apoptosis of chronic lymphocytic leukemia cells through activation of the p53/miR-34a/SIRT1 tumor suppressor network. *Cancer Res*. 2011;71(13):4473–4483.
34. Haigis MC, et al. SIRT4 inhibits glutamate dehydrogenase and opposes the effects of calorie restriction in pancreatic beta cells. *Cell*. 2006;126(5):941–954.
35. Lombard DB, et al. Mammalian Sir2 homolog SIRT3 regulates global mitochondrial lysine acety-

lation. *Mol Cell Biol*. 2007;27(24):8807–8814.
36. Knip M, et al. Safety of high-dose nicotinamide: a review. *Diabetologia*. 2000;43(11):1337–1345.
37. Bhunia AK, et al. PKD1 induces p21(waf1) and regulation of the cell cycle via direct activation of the JAK-STAT signaling pathway in a process requiring PKD2. *Cell*. 2002;109(2):157–168.
38. Li X, Luo Y, Starremans PG, McNamara CA, Pei Y, Zhou J. Polycystin-1 and polycystin-2 regulate the cell cycle through the helix-loop-helix inhibitor Id2. *Nat Cell Biol*. 2005;7(12):1202–1212.
39. Harbour JW, Dean DC. The Rb/E2F pathway: expanding roles and emerging paradigms. *Genes Dev*. 2000;14(19):2393–2409.
40. Zhu L. Tumour suppressor retinoblastoma protein Rb: a transcriptional regulator. *Eur J Cancer*. 2005;41(16):2415–2427.
41. Edelstein CL. Mammalian target of rapamycin and caspase inhibitors in polycystic kidney disease. *Clin J Am Soc Nephrol*. 2008;3(4):1219–1226.
42. Shibazaki S, et al. Cyst formation and activation of the extracellular regulated kinase pathway after kidney specific inactivation of Pkd1. *Hum Mol Genet*. 2008;17(11):1505–1516.
43. Wei F, et al. Neutrophil gelatinase-associated lipocalin suppresses cyst growth by Pkd1 null cells in vitro and in vivo. *Kidney Int*. 2008; 74(10):1310–1318.
44. Hasegawa K, et al. Sirt1 protects against oxidative stress-induced renal tubular cell apoptosis by the bidirectional regulation of catalase expression. *Biochem Biophys Res Commun*. 2008;372(1):51–56.
45. Yeung F, et al. Modulation of NF-kappaB-dependent transcription and cell survival by the SIRT1 deacetylase. *EMBO J*. 2004;23(12):2369–2380.
46. Zhu X, et al. Activation of Sirt1 by resveratrol inhibits TNF-alpha induced inflammation in fibroblasts. *PLoS One*. 2011;6(11):e27081.
47. Busch F, Mobasheri A, Shayan P, Stahlmann R, Shakibaei M. Sirt-1 is required for the inhibition of apoptosis and inflammatory responses in human tenocytes. *J Biol Chem*. 2012;287(31):25770–25781.
48. Nauli SM, et al. Polycystins 1 and 2 mediate mechanosensation in the primary cilium of kidney cells. *Nat Genet*. 2003;33(2):129–137.
49. Nemoto S, Fergusson MM, Finkel T. SIRT1 functionally interacts with the metabolic regulator and transcriptional coactivator PGC-1{alpha}. *J Biol Chem*. 2005;280(16):16456–16460.
50. Battini L, et al. Loss of polycystin-1 causes centrosome amplification and genomic instability. *Hum Mol Genet*. 2008;17(18):2819–2833.
51. Lu W, et al. Comparison of Pkd1-targeted mutants reveals that loss of polycystin-1 causes cystogenesis and bone defects. *Hum Mol Genet*. 2001;10(21):2385–2396.
52. Shao X, Somlo S, Igarashi P. Epithelial-specific Cre/lox recombination in the developing kidney and genitourinary tract. *J Am Soc Nephrol*. 2002;13(7):1837–1846.
53. Ferreira RG, et al. Neutrophil recruitment is inhibited by nicotinamide in experimental pleurisy in mice. *Eur J Pharmacol*. 2012;685(1–3):198–204.
54. Liu D, Gharavi R, Pitta M, Gleichmann M, Mattson MP. Nicotinamide prevents NAD+ depletion and protects neurons against excitotoxicity and cerebral ischemia: NAD+ consumption by SIRT1 may endanger energetically compromised neurons. *Neuromolecular Med*. 2009;11(1):28–42.
55. Shi Y, et al. Protective effects of nicotinamide against acetaminophen-induced acute liver injury. *Int Immunopharmacol*. 2012;14(4):530–537.
56. Green KN, et al. Nicotinamide restores cognition in Alzheimer's disease transgenic mice via a mechanism involving sirtuin inhibition and selective reduction of Thr231-phosphotau. *J Neurosci*. 2008;28(45):11500–11510.
57. Petley A, Macklin B, Renwick AG, Wilkin TJ. The pharmacokinetics of nicotinamide in humans and rodents. *Diabetes*. 1995;44(2):152–155.
58. Takiar V, et al. Activating AMP-activated protein kinase (AMPK) slows renal cystogenesis. *Proc Natl Acad Sci U S A*. 2011;108(6):2462–2467.
59. Happe H, et al. Cyst expansion and regression in a mouse model of polycystic kidney disease [published online ahead of print March 6, 2013]. *Kidney Int*. doi:10.1038/ki.2013.13.